Università degli Studi di Padova

Dipartimento di Scienze storiche, Geografiche e dell'Antichità

Corso di Laurea Magistrale in

Local Development

Assessment of flood hazard susceptibility in South Sudan's Upper Nile state using GIS-based multi-criteria analysis

Relatore: Prof.ssa SILVIA E. PIOVAN

Correlatore: Prof.ssa MICHAEL E. HODGSON

Laureando: MOSES PETER GORDON WANI

Matricola: 2041232

ANNO ACCADEMICO

2022 – 2023

Il candidato dichiara che il presente lavoro è originale e non è già stato sottoposto, in tutto o in parte, per il conseguimento di un titolo accademico in altre Università italiane o straniere.

Il candidato dichiara altresì che tutti i materiali utilizzati durante la preparazione dell'elaborato sono stati indicati nel testo e nella sezione "Riferimenti bibliografici" e che le eventuali citazioni testuali sono individuabili attraverso l'esplicito richiamo alla pubblicazione originale.

The candidate declares that the present work is original and has not already been submitted, totally or in part, for the purposes of attaining an academic degree in other Italian or foreign universities.

The candidate also declares that all the materials used during the preparation of the thesis have been explicitly indicated in the text and in the section "Bibliographical references" and that any textual citations can be identified through an explicit reference to the original publication.

Student's signature

_____

FOR JAMES DAVID VENCE

river subtracted for its
own presence a river run
aground secretly working
as all rivers the double
edge of every beginning
blacked out in concrete pipes

where flood is defenceless
where water level the difference

digging the foundation it's
as though no-one remembers
the water the ground is full
of it pumped out only to
rise up through the mud alive.
By Skoulding (2019)

INDEX

LIST OF FIGURES

LIST OF TABLES

1. INTRODUCTION

1.1. Background and motivation

Floods[1] are among the most ruinous of all natural hazards, conceded to have devastating, immeasurable, and often irreversible impacts. Accounting for one-third of all global natural disasters both in terms of frequency and economic effects (Berz, 2000), floods do inflict severe damages to physical, social, and economic structures, resulting in the disruption of livelihoods around the globe. Statistics from the Emergency Events Database (EM-DAT) curated by the Centre for Research on the Epidemiology of Disasters (CRED) in Brussels shows that, over the last decade alone, there were a total of 1,733 flood events globally (www.emdat.be), impacting an average of 69.43 million individuals (Ritchie et al., 2022). Analysis of trends has further revealed that the number of major flood events has increased significantly over the past decades (Milly et al., 2002; Najibi & Devineni, 2018). Moreover, future projections suggest that the present trend is likely to take an upward trajectory toward more frequent and intense flood events throughout the twenty-first century (Hirabayashi et al., 2008; Kundzewicz et al., 2014; Hirabayashi et al., 2021).

While it is evident that the count of fatalities resulting from flood disasters has exhibited decreased when contrasted with figures recorded per flood event during the 1980s and 1990s (Kourgialas & Karatzas, 2011), the current increase in the frequency and severity of flood disaster, mainly due to climate change-induced climate variations and extreme weather events (Visser et al., 2014), as well as anthropogenic interventions; these are, change in land use, urban growth, and alteration of water courses among other interventions, have raised alarms about the complex impacts floods disasters can have on health, the environment, and socio-economic development, particularly of vulnerable nations and communities as well as the pressing need for initiative to reduce these adverse effects and the possible dangerous consequences. To mitigate the possible dangerous consequences of flood disasters, it becomes important to recognise that the present trend and future flood hazards scenarios necessitates a comprehensive spatial and temporal information regarding the inherent risk associated with flooding (Ouma & Tateishi, 2014).

---

[1] "The unusual accumulations of the water above the ground caused by high tide, heavy rain, melting snow or rapid runoff from artificially paved areas" (Michael, 2006, p.205).

Many countries possess a well-defined legislative framework and legal provision governing the practice of flood hazard and risk mapping (Degiorgis et al., 2012). The oldest known among these legislative measures is the *Flood Disaster Protection Act of 1975*, which acknowledged the significance of flood hazards and mandated the delineation of floodplains and associated hazard zones in the United States of America. Contemporary examples include the *EU Floods Directive (2007/60/EC),* which mandates member state to produce maps detailing flood hazards and risks, the *South African Disaster Management Act No. 57 of 2002*–to mention a few. These forms of regulatory framework represent an indispensable component of flood risk management. They encompass not just the creation and a regular upkeep of flood hazard and risk maps but also establish standardised methodologies, data sources, and reporting mechanisms. These measures are vital in upholding the precision, reliability and comparability of flood hazard and risk maps in facilitating well-informed decision-making (Cirillo & Albrecht, 2015), taking into account the three main components of flood risk management – risk analysis, risk assessment, and risk reduction (Schanze, 2006).

However, while flood hazard mapping and modelling is an integral part of an integrated flood risk management that addresses both the probability and consequence of floods and is widely applied in most developed countries, the situation differs significantly in developing countries. "Flood disaster management in developing countries is mostly reactive responding to prevailing disaster situations–emergency response and recovery" (Islam et al., 2016, p. 31). Despite the growing recommendation for integrated risk-based management that entails a thorough understanding of flood hazards and vulnerabilities, in general sense, investments in developing countries tend to emphasis on post-disaster recovery rather than the establishment of proper adaptive capacities (Mirza, 2003).

Flood hazard mapping remains relatively less prevalent in developing countries–a circumstance attributed to many factors. One of these factors as highlighted in the literature, is the absence of quality dataset (Nkwunonwo et al., 2020). Although the advancement in geospatial and remote sensing technologies exemplified by the lunch of *sentinel-1 satellite* that provides radar-based images for flood hazard mapping along other functions, globally available topographic data such as Shuttle Rader Topographic Mission (SRTM), and particularly for Africa, *the African Regional Data Cube[2],* offers viable remedies to address the challenge of

---

[2] The African Regional Data Cube is an initiative launched in 2018 and overseen by the Global Partnership for Sustainable Development Data (GPSDD) to confront the challenge of data scarcity through the support and provision of quality geospatial data and capacity building in five African countries: Ghana, Kenya, Senegal, Sierra

data paucity, "the limited availability of data and limited access to data are still prevailing issues which now prompt the need for enterprise investment and political discussions" (Nkwunonwo et al., 2020, p. 4). Furthermore, accompanying these challenges is the deficiency in technical expertise and the inadequate infrastructure to efficiently access and harness the potential advantage offered by these datasets–obstacles that are caused by multitude of factors ranging from insufficient funding to political influence (ActionAid, 2006).

Similar to many developing nations, South Sudan faces a significant absence of institutional directives concerning flood hazard mapping. The lack of flood hazard maps stems from factors such as deficiency in technical expertise, limited access to or lack of high-quality dataset, and inadequate resources allocation. These factors collectively have negatively impacted the effectiveness of flood risk mitigation strategies in the country.

To this end, this study addresses this critical challenge with specific focus on the Upper Nile state in the northeastern part South Sudan. This study adopts an integrated approach that harnesses the capabilities of geographic information system (GIS), analytical hierarchy process, remote sensing derived parameters, conventional data, and experts' judgment for flood hazard susceptibility mapping. The primary objective of the study is to gain a clear understanding of the spatial distribution of flood hazard and the various contributing factors that underlie flood occurrence in the Upper Nile state. Seeking to bridge the existing knowledge gab, the generated map is anticipated to provide invaluable insights for improved flood risk management strategies for Upper Nile state.

1.2. Problem statement

South Sudan has experienced a variation in climatic pattern in the past years, ranging from severe drought to periods of above-average rainfall. According to a recent report from the Greater Horn of Africa Climate Outlook Forum, there has been a notable increase in annual average rainfall across the Horn of Africa, with all regions anticipated to continue experiencing above average rainfall in the years ahead (GHOACOF, 2023). The increase in rainfall, both in neighbouring countries and in local context, exerts a substantial influence on the annual

---

Leone, and Tanzania. At present, the initiative is under transition from country-specific–donating the five countries mentioned above–to a broader continental scale known as Digital Earth Africa. Through this transition, the initiative is anticipated to deliver a wide array of solutions encompassing high quality geospatial data, advance tools, and the acquisition of essential skills to achieve the sustainable development goals in African countries (www.digitalearthafrica.org).

discharge of the River Nile (Moon & Hannachi, 2021). Consequently, this intensifies the occurrence of seasonal fluvial and pluvial floods.

Indeed, the last three years have witnessed unusual incidence of flood throughout South Sudan, with the Upper Nile Region (Jonglei State, Unity, Upper Nile, and Pibor Administrative Area) experiencing the most substantial impact. The increase in the frequency and magnitude of flood events has resulted in considerable upheavals within the local communities, causing substantial population displacement. Moreover, the adverse impacts of flooding have been exacerbated due to the absence of holistic flood risk reduction strategies. The existing measures aimed at addressing the challenges of flood disaster are primarily reactive in nature, concentrating on responding to ongoing disaster scenarios.

Although it is acknowledged that the occurrence of flood hazards cannot be prevented, as Rahman et al. (2019) noted, the resultant damages and the adverse effects of flooding can be mitigated, or at the very least substantially reduced through the precise pre-identification of flood-prone areas before the onset of flooding events. As such, it is fundamental to assess the susceptibility of Upper Nile state to flood hazards and identify the levels of risk associated with flooding in various areas within Upper Nile state. This assessment is a crucial component upon which to formulate measures and strategies aimed at mitigating flood-related risks.

1.3. Objectives and significance of the research

This study focuses on the understanding of the geographic extent of floods and the impact of various factors contributing to flood events in the Upper Nile state. Its primary goal is to meticulously evaluate and identify areas within the study that probabilistically may experience inundation in the event of flood occurrence. In other words, the study examines the potential spatial extent of floodwater within the boundaries of study area during flood scenarios. Through a cartographic approach, the study specifically aims to delineate the study area into five distinctive zones contingent upon their probability of being submerged during flood events. Herein, and depending on the unaccounted variable of flood water volume, the study classifies areas that may experience inundation with minimal increase in the volume of water inflow, mainly due to its localised topographical, hydrological, and climatic characteristics as very highly and highly susceptible to flood hazard; and conversely, areas that may not experience inundation as having a very low or low susceptibility rate. Therefore, using GIS-

Based multi-criteria decision-making and the analytical hierarchy process, the study addresses several key inquiries, including:

- Identification of factors influencing flooding events in the Upper Nile state;
- determination of the relative importance of the factors in flood hazard mapping;
- determination of flood susceptibility level in the Upper Nile state of South Sudan, ranging from very low to very high susceptibility level to flood hazards (FHZs);
- and the examination of the type of land use/land cover that falls within various zones with different susceptibility level to flood hazards.

Given these considerations, this study aims at providing a clear information on the potential flooding zones in the Upper Nile state, with the ultimate objective of [1] developing flood hazard map for Upper Nile state, that [2] assesses the risk level of various areas and [3] provides a detailed analysis of the various land use types at the risk of flood hazards. By implementing the first component of flood risk assessment–identification of areas prone to flood hazards and level of exposure–, the outcome of the study is expected to be an invaluable instrument for the formulation of pre-flood preparedness measures and risk mitigation strategies.

1.4. Scope and limitations of the research

An in-depth comprehension of flood hazards constitutes a fundamental component in addressing flood-related disasters and associated risks. A thorough apprehension of flood hazards and the development of impactful mitigation and adaptation strategies thus requires a detail information on the spatial and temporal dimensions of the hazard. These entails the examination of the geographic extent of the hazards, including scope and boundaries of inundation; topographical, hydrological, and anthropogenic factors influencing flood occurrence; frequency and depth of flood hazard, including the intensity and volume of Surface runoff; as well as the exposure and vulnerability level of various entities.

Although these elements are interconnected and all together forms the basis of integrated flood risk management, the current study is centred solely on assessing the potential geographic extent of flooding in the study area, with specific emphasis on delineating areas susceptible to flood hazards.

The study lacks an incorporation of the temporal dimension in evaluating flood hazards, specifically, the identification of elements such as frequency, intensity, depth, and volume of

surface runoff. These have been excluded from the analysis due to their dependence on extensive datasets such as annual peak discharge records and flood flow frequency guidelines both which are lacking for the area under investigation mainly due to limited historical observational data, and institutional constraints.

Despite the attempt to encompass the vulnerability and exposure components within the evaluation of flood hazard in this study, it is crucial to acknowledge that this attempt is particularly without depth and is centred only on the different types of land use/ land-cover that are potentially susceptible to inundation during flood scenarios. Therefore, it is imperative to view this study as a guide for future research endeavours that systematically account for the temporal dimension of flood hazards as well the vulnerability of the local population to flood disaster and related risks in the Upper Nile state.

1.5. State of the art

4.2.3. An Overview of Flood Hazard Mapping

In *flood risk management*[3], the basic and yet crucial element of evaluating flood hazards involves drawing upon historical flood records, hydrological, meteorological, and topographical information, a comprehensive spatial and temporal details on the potential risk of flooding. This processes known as *flood susceptibility mapping and flood frequency analysis* [4] is an integral component of *flood risk analysis*[5] within the broader frame of flood risk management. The first aspect known as flood hazard mapping, facilitates the precise delineation of the spatial extent of potential flood hazards, and the spatial distribution of related risk. Recognising its critical importance, the identification of the spatial extent of flood hazards, coupled with the implementation of appropriate mitigation measures, has the potential to greatly reduce the impact of flood events. As such, flood hazard mapping and flood hazard maps play a crucial role in various management practices, including land use

---

[3] "A holistic and continuous societal analysis, assessment and reduction of flood risk" (Schanze, 2006 p.4).
[4] "Flood susceptibility mapping can be defined as a quantitative or qualitative assessment of the classification, area, and spatial distribution of flood, which exists or potentially may occur in an area" (Rahman et al., 2019). Whereas flood frequency analysis is "a technique commonly used to relate the magnitude of extreme runoff or river flow events to their frequency of occurrence through the use of probability distribution functions" (Moges & Taye, 2019, p. 386).
[5] Flood risk is defined as the likelihood of adverse outcomes resulting from floods and is contingent upon the exposure of elements at risk to flood hazards. flood risk analysis on the other hand, is the determination of past, current or – based on proposed activities or uncontrollable trends (global change) – future risks (Schanze, 2006).

planning, water resources planning, the development of early warning systems, and the design of emergency response strategies in the event of flooding (Naulin et al., 2013; Zhang & Chen, 2019; Allafta & Opp, 2021).

Over the past and in recent years, significant efforts have been devoted to understanding, forecasting, and analysing flood hazards and the underlie adverse effects across various scales, spanning from a single structure to neighbourhoods, cities, regions and even the global scale. The systematic effort within the research community have resulted into the development of a variety of modelling techniques, significantly improving the capability of flood hazard mapping (Teng et al., 2017). Various types of models have been proposed by researchers to assess flood hazards and according to Mudashiru et al. (2021), these models can be classified into three broad categories: namely, the physically-based, physical modelling, and empirical methods, illustrated in Figure 1.

1.5..1. Physically-Based Modelling

The Physically-based modelling are numerical techniques that reproduce the physical process of water flow using various data inputs, such as hydrological parameters, river network geometry, topographic information, and remote sensing data to stimulate hydrological processes contributing to flood events (Mudashiru et al., 2021). Physical-based modelling consist of numerical models, often referred to as hydrodynamic models that uses measurable variables and variables defined by time and space to solve flow equation in 1-, 2-, and 3-D dimensions by applying the principles of physics–mass, energy, and momentum. Numerical models are widely use in stimulating flood dynamics, flood forecasting and scenario analysis, and can mitigate numerous limitations associated with the physical and empirical models due to their utilisation of inputs having physical interpretation (Devia et al., 2015). For instance, unlike empirical models, physically-based models offer the flexibility to adjust their input variables, enabling the evaluation of impacts resulting from changes in initial conditions, boundary conditions or topographic data, thereby integrating changes in hydraulic features or structures (Teng et al., 2017). However,–a challenge commonly encountered when modelling physical processes–there is empirical evidence indicating error and uncertainty associated with physically-based models in deriving model parameters from terrain (Y. Chen et al., 2016), and substantial differences in modelling outcomes (Neelz & Pender, 2013), as well as the limitation of these models in reproducing the intricate dynamics of complex flows (Carmo, 2020).

1.5.1.1. Physical Modelling

Physical modelling represents resource-intensive experimental techniques with the capacity to retrospectively analyse historical flood events and predict the extent of future flood events (Mudashiru et al., 2021). This is achieved through the application of precise equations that are systematically solved to stimulate real-world flood scenarios experimentally. Physical modelling methods were widely used in flood hazard mapping up until the 1970s. However, the high cost implication, time, and experimental demands of this modelling techniques coupled with the advancement of robust numerical models capable of replicating the physical aspect of fluid flow have driven the transition from physical models to numerical models (Bellos, 2012). The application of numerical models to depict physical processes have greatly diminished the necessity for physical models. The shift to numerical models, however, does not signify the abandonment of physical modelling. As Bellos (2012) noted, a numerical model cannot be deemed validated unless it has been subjected to comparison with at least one experiment. As such, physical models are still in use as benchmark test for numerical models as well as for practical aspect where the studied phenomenon cannot be stimulated numerically.

1.5.1.1. Empirical Methods

Empirical modelling techniques represents data-driven models that exclusively relies on observational data (Devia et al., 2015). These models use mathematical equations derived from simultaneous input and output time series, as opposed to the physical process within a catchment, and their applicability is limited to the catchment boundaries. Based on their respective approaches, empirical models can be classified into quantitative and qualitative methods. The quantitative empirical models are based on the numerical expression between flood occurrence and flood controlling/contributing factors (Wang et al., 2011), while qualitative models depends on experts' opinion. Conversely, certain qualitative approaches, such as the Multi-Criteria Decision Analysis that involve the empirical derivation of ranks and weights can become semi-quantitative in nature. further classification of empirical models encompasses the statistical methodologies which includes bivariate (Costache, 2019) and multivariate (Tien Bui et al., 2019) models, machine learning (Rahman et al., 2019) and the artificial intelligence approaches, and the Multi-Criteria Decision (Allafta & Opp, 2021) Analysis, which is utilised in this study and will be extensively elaborated upon in the next subsection. "Flood prediction through empirical modelling strives to create a connection between the physical processes which encompasses flood generation through regression

equations and parameters that are capable of evaluating flood frequency analysis or flood spatial extent" (Mudashiru et al., 2021, p. 8). This is accomplished through the utilisation of wide range of data sources, including hydrological, topographical, geomorphological and Digital Elevation Models (DEM), often obtained using remote sensing techniques and subsequently processed within Geographic Information System (GIS) environment (Wang et al., 2018).
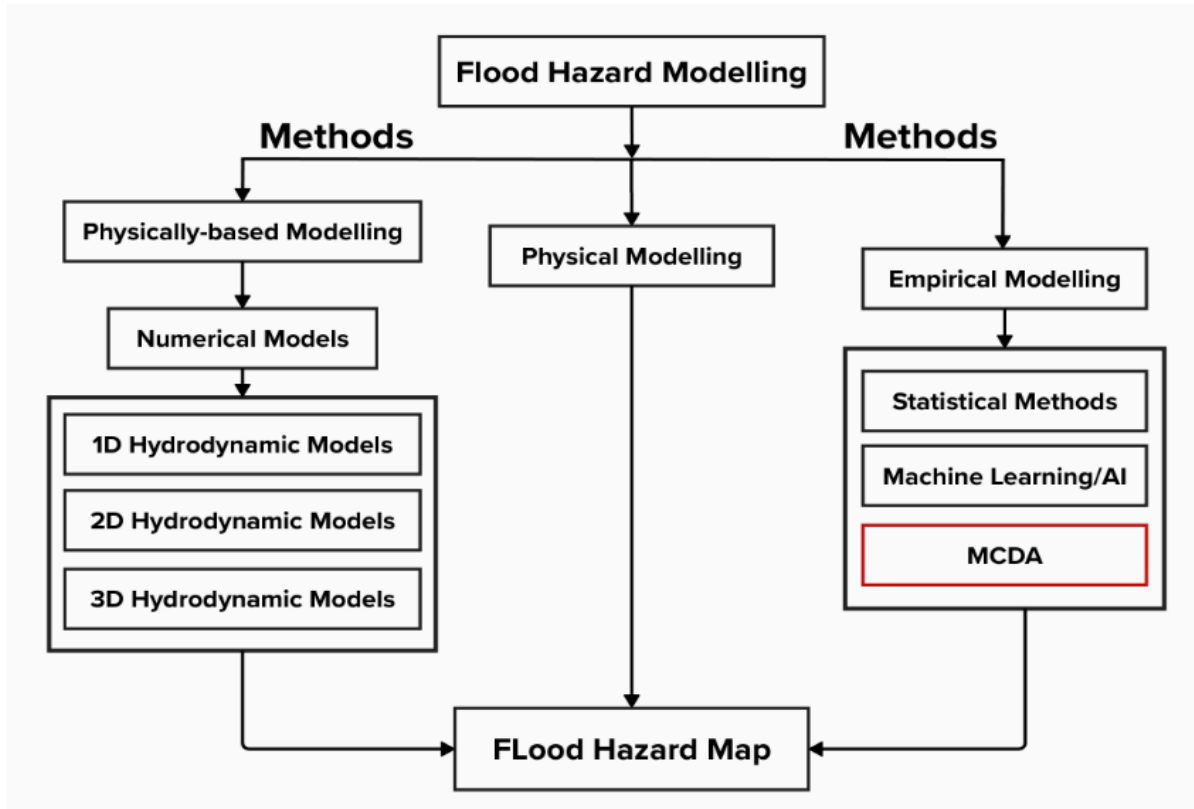
Figure 1. A schematic graphic depicting the methodological process encompassing the three categories of flood hazard modelling techniques.

1.5.2. Multi-Criteria Decision Analysis

Multi-Criteria Decision Analysis (MCDA) is a collection of decision-making approaches that involves set of alternatives used in solving complex decision problems of conflicting and incommensurate evaluation criteria (Malczewski, 2006; Malczewski & Rinner, 2015; de Brito & Evers, 2016). MCDA enables decision-makers to integrate multiple information thereby easing decision-making processes, typically resulting in a set of weights linked to range of objectives. A multicriteria decision problem relies on three fundamental components; these are, 'decision-making entity' which holds the responsibility of making decision and can be an individual, a collective group or an organisation, 'criteria' that have properties (comprising of attributes and objectives) to depict the multifaceted nature of the decision context, and

'decision alternatives', which present different courses of action from which the decision-making entity is obliged to select. These components along with other fundamental principles, – *value scaling, criterion weighting, and combination rule*[6] – serves as foundational elements upon which the methodologies for addressing spatial and non-spatial multicriteria problems are constructed.

The development of GIS-MCDA paradigm, related methods, and models, find it origin in two distinct research traditions (Malczewski & Rinner, 2015). These research traditions are Operation Research, a discipline known for the application of mathematical-based problem-solving methods and approaches in decision making, and landscape architecture and spatial planning, a discipline characterised by its systematic approach in examining physical and non-physical conditions, and the application of scientific principles in the planning, designing, and managing of natural and built environments. Within Operation Research tradition, the contributions of F.Y. Edgeworth and V. Pareto i.e., the introduction of an approach for combining conflicting criteria into a single evaluation index, and Pareto's introduction of the notion 'efficiency' as pointed out by Malczewski and Rinner (2015), serves as the early foundation of today's GIS-MCDA. Furthermore, Von Neumann and Morgenstern (1947) introduction of 'expected utility theory' and 'axiom of rationality', Churchman et al. (1957) application of simple additive weighting methods in solving multicriteria problem, Roy (1968) and related associates' development of MCDA method based on the idea of outranking relations, set a foundation for early MCDA Approaches.

In the field of landscape architecture and spatial planning, the earliest contributions can be attributed to American architects, notably, C. Eliot and W. Manning during the later part of nineteenth century and earlier decades of the twentieth century (Collins et al., 2001). Their exposition of the overlay technique, along with the application of the method on hand-drawn maps, which was later advanced by McHarg (McHarg, 1969) through the use of transparent map overlay approach to land-use suitability analysis constitute the foundational stages in the development of complex GIS-MCDA methodologies.

---

[6] In MCDA methods, the criteria used for evaluating alternatives are required to be standardized. This is achieved through a process known as 'value scaling' in which row data is converted into comparable units. Once each criterion has been transformed, it is assigned a weight (criterion weighing) that represents its relative importance. Following 'combination rule', these weighted criteria are then integrated with information about the alternatives and the deciding entity's preference, resulting in an overall assessment of the alternatives (Malczewski & Rinner, 2015).

Throughout the course of 1960s, multitude of MCDA methods were developed (Mendoza & Martins, 2006) and by 1990s, - GIS-MCDA solidified its status as a distinct research domain within the GIScience literature, a pivotal progress that laid the groundwork for the emergence of spatial decision support paradigm (Malczewski, 1999). This decade was followed by years of proliferation in the application of GIS-MCDA approaches across a diverse range of decision-making and management scenarios, including the selection of optimal strategies for flood risk mitigation (Tkach & Simonovic, 1997), and the assessment of index-based flood hazards, with an emphasis on the factors that influence flood occurrence (Kourgialas & Karatzas, 2011; Kazakis et al., 2015; Arabameri et al., 2019a).

1.5.2.1. GIS-MCDA Methodologies in Flood Hazard Mapping

This sub-section provides a brief description of various multi-criteria decision methodologies used in the context of flood hazard mapping. It is crucial to emphasise that the methods briefly represented herein does not encompass the entire array of available MCDA methodologies for flood hazard mapping. Selection of the approaches outlined here is based on the prevalence and significance of these approaches in flood hazard mapping, as substantiated by existing body of literature provided in Table 1.

A. Analytical Hierarchy Process (AHP)

Among the multitude of MCDA methods, the analytical hierarchy process stands out as one of the most widely used method in flood hazard mapping (Mahmoud & Gan, 2018). This method is based on three fundamental principles: (1) decomposition, a procedure necessitating a systematic breakdown of a decision problem into a hierarchical structure that effectively captures the fundamental components inherent to the problem; (2) comparative judgment, referring to a pairwise comparison of the components within a specific level of the hierarchical structure, taking into account the components at the high level of the structure; and (3) synthesis of priorities, entailing a construction of an overall priority rating. Studies that have examined the MCDA literature have reveal that, a predominant trend among studies utilising MCDA methodology usually involves the integration of MCDA with the analytical hierarchy process method (Wang et al., 2011; de Brito & Evers, 2016). Indeed, the analytical hierarchy process method prove to be an effective technique especially when integrated with GIS based multicriteria analysis in solving complex spatial problems.

B. Analytical Network Process (ANP)

This method represents an extension and a generalised form of the analytical hierarchy process (Malczewski & Rinner, 2015). Introduced by Saaty (1996), this methodology addresses

decision problems in the context of dependencies among the constituent components of decision situation. The underlying assumption is that real-world spatial decisions encompass intricate pattern of interaction and interdependence among component of the decision problem and therefore, an emphasis on the interdependencies among the evaluation criteria is necessary in assessing decision alternatives. While this methodology adheres to the same principles of the analytical hierarchy processes, it diverges from AHP in terms of its approach to the principle of decomposition; i.e., decomposition in analytical network process entails the structural organisation of decision problem through network framework rather than a hierarchical one. Dano et al. (2019) reported a high reliability of the analytical network process in discerning the interconnections among real-world factors such as those influencing flood occurrences.

C. Fuzzy-AHP

The Fuzzy AHP is a technique introduced to reduce the uncertainty associated with the Analytical Hierarchy Process due to its subjective nature. "It enables expert's judgment to be defined through means of fuzzy numbers based on the concept that decision-making by humans is associated with uncertainties that are difficult to explain by single numbers" (Mudashiru et al., 2021, p. 9). Among the various types of Fuzzy AHP, the trapezoidal fuzzy AHP and the Triangular Fuzzy AHP are commonly used in flood hazard mapping.

D. TOPSIS

Technique for Order of Preference by Similarity to Ideal Solution (TOPSIS) is a method based on the concept that the preferred alternative is distinguished by its closest proximity to the most immediate positive ideal solution and its furthest distance from the negative ideal solution. According to Moghadas et al. (2019), this method is a valuable instrument for decision-makers as it facilitates the effective integration of flood mitigation planning by means of a comprehensive flood hazard analysis, particularly for Urban areas.

E. Fuzzy-TOPSIS

Initially, this approach was conceived based on the theoretical underpinnings of fuzzy set theory, with the specific aim of providing resolutory insights to the intricate issue of supplier selection within the field of supply chain management (Chen et al., 2006). Subsequently, Kim et al. (2019) drew attention to the viability of using a hybrid fuzzy TOPSIS approach for flood hazard mapping, taking into account the uncertainties involved when developing flood hazard maps for levee failure. Their findings suggest that the approach is significantly advantageous, particularly in terms of enhancing accuracy in the classification of flood-prone areas. This was

further substantiated by research that ascertained the efficacy of fuzzy TOPSIS approach in the context of decision-making related to flood and water resources management (see; Lee et al., 2014).

F. DEMATEL

Decision-making trial and evaluation laboratory (DEMATEL) is designed for a comprehensive and systematic analysis of complex decision problems that are interconnected and interdependent (Wang et al., 2018). This approach facilitates a thorough examination of the complexities inherent in any multifaceted decision scenario, enabling a comprehensive understanding of the underlying intricacies and interactions. According to Kanani-Sadat et al. (2019), this method is a preferable in mapping flood hazards, particularly for data-scarce and ungauged regions due to its networking and interdependencies of criteria.

G. VIKOR

VIKOR (VlseKriterijumska Optimizacija I Kompromisno Resenje), a multi-criteria optimisation and compromise solution is an approach that "uses aggregating function and focuses on determining compromising solutions for a prioritisation problem with conflicting criteria" (de Brito & Evers, 2016, p. 4). In essence, the method enhances multi-criteria decision-making, particularly when faced with the complex task of assigning priorities to various alternatives while taking into account the inherent conflicts among the criteria used in any given analysis. In an study that evaluates predictive capacity of multi-criteria decision methods and other machine learning methods, Khosravi et al. (2019) found that VIKOR, similar to other MCDM has flood prediction capabilities greater than 95 %, indicating the promising nature of this method in the assessment of areas susceptible to flood events.

1.5.3. Case Studies

Herein, several studies that conducted flood hazard mapping using GIS-based Multicriteria decision analysis and the Analytical hierarchy process (AHP) are briefly discussed. Although the scope of the discussion is not exhaustive and limited to include only studies that have integrated GIS-MCDA with the analytical hierarchy process (AHP), in the interest of providing a relatively comprehensive overview of the literature, **Error! Reference source not found.** present a concise list of studies that utilised different GIS-MCDA methodologies together with other modelling techniques in mapping flood hazards. The literature presented in **Error! Reference source not found.** shows the application of MCDA and other flood hazard mapping techniques in different parts of the globe. The Methods applied in those studies are diverse in

nature, including: AHP = Analytical hierarchy process; ANP = Analytical network process; WLC = Weighted Linear combination; F'AHP = Fuzzy analytical hierarchy process; TOPSIS = Technique for Order of Preference by Similarity to Ideal Solution; F'TOPSIS = Fuzzy Technique for Order of Preference by Similarity to Ideal Solution. Methods that weren't specified and generically labelled as others in **Error! Reference source not found.** encompasses MCDA techniques such as Decision-making trial and evaluation laboratory, which accounts for the complexities inherent in any multifaceted decision scenario; VlseKriterijumska Optimizacija I Kompromisno Resenje, which aggregates functions and is based on compromising solutions for a prioritisation problem with conflicting criteria. Furthermore, the literature provided in **Error! Reference source not found.** also utilised non-MCDA techniques as those mentioned in subsection **4.2.3**. Notably, machine learning and artificial intelligence approaches; statistical approaches such as bivariate and multivariate models in flood hazard mapping.

One of the earliest application of multicriteria decision analysis in flood-related studies can be attributed to Levy (2005). The researcher introduced a decision support system based on the analytical network process to address flood planning and management problem in the middle reaches of the Yangtze River, China. The finding from his investigation stressed the considerable potential of Decision Support System and Multi-Criteria Decision Analysis in improving flood risk planning and management, particularly in scenarios characterized by uncertainties and complexities. Similarly, Le Cozannet et al. (2013) assess the suitability and utility of multi-criteria decision analysis, specifically the analytical hierarchy process in mapping the physical vulnerability of coastal areas to flooding and erosion through its application in two coastal areas in France–Languedoc-Roussillon and the island of La Réunion. The result of analysis aligned with researchers' initial assumptions, revealing a heightened vulnerability in both areas as well as the effectiveness of the analytical hierarchy process in providing a flexible and transportable framework to support long-term coastal zone planning and adaptation measures to flood events.

Chen et al. (2014) employed the analytical hierarchy process to assign relative weights to indices derived from climate, hydrological, topographical, vegetation, and soils data, with the ultimate objective of creating a spatial multi-criteria decision making (SMCDM) framework designed for the assessment of flooding risk at regional scale using part of the Bowen Basin in Queensland, Australia as a study area. The regional flood map they developed was validated through a comparison with satellite-derived inundation map. The analytical hierarchy process as the researchers noted, produced a highly accurate results and efficient in the assessment

of flooding risk on a regional scale. Similarly, Kazakis et al. (2015) adopted the MCDA-AHP approach to assign weights to seven distinctive and conflicting criteria influencing flood occurrence. The values they attained and related individual maps were superimposed in GIS, resulting into flood hazard map for Rhodope–Evros region, Greece. To further assess the accuracy of the method, the researchers conducted a sensitivity analysis using 'effective weight' technique. The sensitivity analysis substantiated the accuracy and reliability of MCDA-AHP approach as well as the identified flood influencing factors in flood hazard mapping at larger (regional) scale.

Elkhrachy (2015) on the other hand, applied MCDA-AHP approach to generate flash flood map for Najran city, Saudi Arabia. Using GIS-based remote sensing and conventional data analysis, Elkhrachy produced flood hazard maps which as he noted, has a crucial role as a reference for carrying out a more detailed examination of flash flood phenomena in Najran city, and the implementation of proper flood risk reduction measures. Gigović et al. (2017) conducted a similar study–urban flood hazard assessment–for Palilula Municipality in Belgrade, Serbia using the analytical hierarchy process. To account for uncertainties in experts' decision, the researchers further applied three different methodologies of the analytical hierarchy process concurrently in different scenarios. Notably, when compared against historical flood inundation data for validation, one of the methodologies the researchers applied–interval rough analytical hierarchy process (IR'AHP)–, exhibited a higher level of compatibility in comparison to the Fuzzy AHP and the conventional crisp AHP. However, it is crucial to emphasise that the other two methodologies–F'AHP and AHP–demonstrated a satisfactory consistency with the spatial distribution and extent of historical flood hazards.

Franci et al. (2016) used the analytical hierarchy process to assign weights to five flood influencing factors in an effort to generate flood susceptibility map for Yialias river basin in Nicosia, Cyprus. The result of their study stresses the efficacy of the MCDA/AHP in flood hazard assessment, particularly in cases where data is limited as well as for conducting a comprehensive analysis over large geographic areas. Similarly, Hagos et al. (2022) identified flood-prone areas in Ethiopia's Teji watershed and upper Awash River basin using GIS based multicriteria-decision method. Their approach involved the application of analytical hierarchy process in assigning weights to seven flood influencing factors selected based on the literature. Their analysis revealed that approximately 55 % of the total areas of the basin fell within the high and extremely high classification of flood hazard zones. To validate their findings, the researchers compared the results of the study with historical maps documenting previous

instance of flood observed in the watershed. The validation analysis showed that, the produced flood hazard map has a high degree of consistency with the previous flood affect areas, thus indicating the reliability and efficiency of MCDA/AHP method in assessing flood prone areas.

Khaleghi and Mahmoodi (2017) generated flood hazard map for Lighvan catchment, Iran. Using MCDA-AHP approach, they examined the complex dynamics of the catchment, taking into consideration various parameters influencing flood risk and vulnerability. The findings from their study subsequently evolved into set of guidelines, providing invaluable guidance for managers and planners in making informed decision concerning management of catchment area to mitigate flood hazard. Similarly, in an effort to developed flood hazard model assessing the susceptibility of the Shatt Al- basin to flooding, Allafta and Opp (2021) adopted multi-criteria decision approach, utilising the analytical hierarchy process to assign relative weights determined by experts to various factors influencing flood events. These factors encompassed rainfall, distance to the river, digital elevation model, slope, land use/land cover, drainage density, soils, and lithology. The researchers further pointed out that the utilisation of GIS-based spatial multi-criteria evaluation framework in conjunction with the analytical hierarchy process can prove to be an effective approach in delineating flood hazard zones. This method's effectiveness as they noted, is evident in its flexibility, ease application, and cost-effectiveness, rendering it a viable method for assessing flood hazards, particularly in regions characterised by scarcity or limited access to data and information.

N.	Literature	APPLICATION LOCALE	AHP	ANP	WLC	F'AHP	TOPSIS	F'TOPSIS	Other
1	Levi (2005)	Yangtze river, China		x					x
2	Raaijmakers et al. (2008)	Ebro Delta, Spain	x						x
3	Lim and Lee (2009)	South Korea							x
4	Kourgialas & Karatzas (2011)	Koiliaris basin, Greece			x				
5	Fernández & Lutz (2010)	Tucumán, Argentina	x		x				
6	Yang et al. (2013)	Yangtze River, China				x			x
7	Le Cozannet et al. (2013)	France	x						
8	Mondlane et al. (2013)	Mozambique	x						
9	Lee et al. (2014)	Han River basin, Korea						x	
10	Chen et al. (2014)	Australia	x						
11	Elkhrachy (2015)	Najran, Saudi Arabia	x						
12	Kazakis et al. (2015)	Rhodope–Evros, Greece	x						
13	Arianpour & Jamali (2015)	Omidieh, Iran	x			x			x
14	Franci et al. (2016)	Nicosia, Cyprus	x						
15	Khaleghi & Mahmoodi (2017)	Lighvan catchment, Iran	x						
16	Gigović et al. (2017)	Belgrade, Serbia	x			x			x
17	Chundeli & Kranthi (2018)	Chennai, India							x
18	Hong et al. (2018)	Poyang County, China				x			x
19	Hategekimana et al. (2018)	Mombasa, Kenya				x			x
20	Sonmez & Bizimana (2018)	Waverly City, Iowa, USA			x				x
21	Liu et al. (2019)	Angkor, Cambodia	x						x
22	Arabameri et al. (2019b)	Kiasar watershed, Iran	x				x		x
23	Khosravi et al. (2019)	Ningdu, China					x		x
24	Moghadas et al. (2019)	Tehran, Iran	x				x		

			Col1	Col2	Col3	Col4	Col5	Col6
25	Rahman et al. (2019)	Bangladesh	x					x
26	Dano et al. (2019)	Perlis, Malaysia		x				
27	Kim et al. (2019)	Gam river, South Korea				x	x	
28	Kanani-Sadat et al. (2019)	Kurdistan province, Iran		x	x			x
29	Feloni et al. (2020)	Attica region, Greece	x		x			
30	Dash & Sar (2020)	India	x					
31	Souissi et al. (2020)	Southeastern Tunisa	x					
32	Morea and Samanta (2020)	Papua New Guinea	x					
33	Abdrabo et al. (2020)	Hurghada, Egypt	x					x
34	Ogato et al. (2020)	Ambo Town, Ethiopia		x				
35	Aladejana (2021)	Owena basin, Benin			x			
36	Vojtek et al. (2021)	Topla basin, Slovakia	x					x
37	Hamlat et al. (2021)	M'zi wadi basin, Algeria	x					
38	Ekmekcioğlu et al. (2021)	Istanbul, Turkey	x				x	
39	Allafta & Opp (2021)	Irak-Iran	x					
40	Ajibade et al. (2021)	Ibadan city, Nigeria	x					x
41	Öztürk et al. (2021)	Corum, Turkey	x					
42	Borzi et al. (2021)	Pampean, Argentina	x					
43	Vaddiraju & Talari (2022)	India	x					
44	Mothapo et al. (2022)	Limpopo, South Africa	x					
45	B. Mudashiru et al. (2022)	Penang, Malaysia	x		x			
46	Gupta & Dixit (2022)	Assam, India	x					
47	Hagos et al. (2022)	Awash basin, Ethiopia	x					
48	Agustina et al. (2023)	Bandung, Indonesia	x					
49	Enomah et al. (2023)	Limbe, Cameroon	x					x
50	Corvacho-Ganahín et al. (2023)	Acha–Arica, Chile	x					x
51	Wijesinghe et al. (2023)	Neluwa, Sri Lanka	x					
52	Ha et al. (2023)	Quang Binh, Vietnam	x					x

Table 1. Literature on the different flood hazard modelling techniques.

2. GEOGRAPHICAL AND HISTORICAL CONTEXT

2.1. The study area: a brief geographical description

The study Area is located in the most northeastern part of South Sudan: known as Upper Nile state, it shares a border Sudan to the north and Ethiopia to the east. Characterised by a vast floodplain, the study area covers an area of about 78,347 square kilometres (Country report, 2015), and forms the northeastern edge of the Upper Nile ecoregion (www.feow.org). To the west of the study, lies the White Nile River stretching from the southwestern corner of the state northward. The White Nile is one of the two main tributaries of the Nile River (the other being the Blue Nile) that originates from Lake Victoria, draining via lake Kyoga to lake Alberta and then Bahr al Jabal, forming at 'Lake No' – the convergence of Bahr al Jabal and Bahr al Ghazal River. The study area is traversed by multiple rivers, a vast network of streams, a large number of minor tributaries, and seasonal watercourses which at times feed and are fed by the main river systems (Johnson, 1986). One of the principal tributary is the Sobat River, a well-known tributary of the White Nile "which draws its water from the Ethiopian plateau and the Pibor river system" (Johnson, 1989, p. 465), stretching for 354 kilometres and pouring into the White Nile at Doleib Hill 16 kilometres south of the city of Malakal (Goes, 2022).

While the topography in the eastern segment–bordering Ethiopia–is mainly composed of highland areas and plateaus, the predominant topographical scenery of the study area is characterized by flatlands with an average elevation of 400 meters above sea level. In terms of physiographic classification, approximately 90 % of the terrain is a part of the eastern flood plain (Acted & Reach, 2013) and the southwestern edges constitutes the Nile-Sobat river which is part of the Sudd swamp. "Most of the soils are clay, virtually impervious to water at the height of the rains, but there are some outcrops of sandier soil, slightly elevated above the plains, where woodland can be found, permanent villages built and cultivation undertaken" (Johnson, 1989, p. 465). The second largest sedimentary basin of the central African rift system lies within the delineated of the study area (Zhao et al., 2020).

The geological aspect on the other hand, is mainly distinguished by three major formations: quaternary-Tertiary unconsolidated sedimentary deposit, Tertiary-quaternary Um Ruwaba formation, and Precambrian crystalline basement rocks (Persits et al., 1997). Unconsolidated sedimentary deposits are composed of well-sorted silts and clays with occasional sandy strata

Figure 2. Geographical location of the study area depicting the boundaries of study area, the main administrative boundaries within the state, main waterbodies, and major road networks.

and are extensively deposited along the White Nile River, major tributary such as Sobat River and other minor tributaries. The Um Ruwaba formation on the other hand, is unconsolidated superficial sediments formed at Late Tertiary to Quaternary with limited stratification consisting of sands, clays, and gravels. "Overlaying the Um Ruwaba sediments are late Pleistocene and Holocene deposits, forming the extensive clay plains of the sudd swamps and

the seasonally flooded areas" (Harvey, 1982, p. 8). Additionally, especially to the southeast part of the study area are undifferentiated basement with granitic intrusions and basic volcanic rocks, which are associated with tectonic activity that formed the Kenyan and Ethiopian rift valleys and the Ethiopian plateau (www.bgs.ac.uk).

According to the Koppen-Geiger classification, the study area is under the influence of two climates, namely Arid Steppe (BSh) and tropical savannah (AW) (Peel et al., 2007). The Arid Steppe (hot) climate is essentially predominant in the north and western part of the study area, characterised by annual mean temperature above 18° C and annual mean rainfall ranging from 250 mm to 600 mm (www.uea.ac.uk). The south and eastern part on the other hand, which is characterised by tropical savannah climate, experiences an annual average rainfall between 800 – 1600 mm annually.

Based on the map produced by the Food and Agriculture Organisation of the United Nations (Figure 3), the landcover pattern within the study area is primarily characterised by natural and semi-natural vegetation areas (FAO, 2011) . The prevailing ecological habitats encompasses grasslands and rangelands with close-to-sparse vegetation such as Herbaceous (HCO: Figure 3) which covers 41.49 % of the entire study area and shrubs (SCO: Figure 3) which accounts for 38.88 % of the study area (FAO, 2011). Other vegetation such as woody perennial plants (TCO: Figure 3) account for 12.75%, followed by agricultural land (denoted as AG: Agriculture in terrestrial and aquatic/regularly flooded land in Figure 3) which represent 6.20 % of the landcover. Approximately, 0.43 % of the land in the study area is covered by seasonal and perennial water (presented as WAT in Figure 3) bodies, 0.17 % by bare rocks and soil or unconsolidated materials (BS: Figure 3), and 0.10 % by artificially built environment – human settlements (URB: Figure 3).

The study area is estimated to have a population of approximately 1.5 million people. The eastern flood plain zone which represents 90 percent of the study area is peculiar for agro-pastoral economy. From an agricultural perspective, the Upper Nile state is one of the largest croplands in South Sudan, accounting for 63 percent of the national cropland area. The principal produce are crops such as Sorghum, maize, cowpeas, and pumpkin seeds. Cattle, goats and sheep are also reared in the zone (Acted & Reach, 2013). The Nile and Sobat Rivers zone on the other hand, have an economy that is primarily based on agriculture and supplemented with fishing, gathering and livestock production (acted & Reach, 2013).

AG Agriculture in terrestrial and aquatic/regularly flooded land	TCO Trees closed-to-sparse in terrestrial and aquatic/regularly flooded land	SCO Shrubs closed-to-sparse in terrestrial and aquatic/regularly flooded land	HCO Herbaceous closed-to-sparse in terrestrial and aquatic/regularly flooded land	URB Urban areas	BS Bare Rocks and Soil and/or Other Unconsolidated Material(s)	WAT Seasonal/perennial, natural/artificial waterbodies	TOTAL AREA
39,169	74,276	259,544	801,428	586	0	3,227	1,178,230
37,368	102,323	70,317	140,993	0	4,747	2,038	357,786
7,192	85,895	439,381	172,974	0	0	0	705,442
28,621	50,386	322,109	121,192	0	0	1,411	523,719
18,879	18,087	691,687	472,183	365	0	228	1,201,429
15,544	102,243	197,532	80,832	0	0	143	396,294
5,739	9,716	5,019	51,785	1,145	0	1,677	75,081
32,305	69,721	404,555	151,338	0	6,626	8,108	672,653
16,021	107,734	132,610	436,211	3,686	0	4,670	700,932
9,963	50,702	149,006	307,743	0	0	4,401	521,815
263,616	153,321	193,126	392,690	2,072	1,717	5,592	1,012,134
11,416	174,062	181,026	119,739	0	90	2,865	489,198
485,833	998,466	3,045,912	3,249,108	7,854	13,180	34,360	7,834,713

Figure 3.   Land cover types of Upper Nile state

22

2.2. Flood pattern in the Upper Nile plain and history of floods

2.2.1. Flood Pattern in the Upper Nile Plain

The geographical region under investigation is situated within the boundaries of the Upper Nile plain, a locale that has exhibited vulnerability to naturally occurring environmental catastrophes spanning millennia. One of these environmental catastrophes is recurring floods. The physical characteristic and the climate of plain, along with those of adjoining territories are known to be the primary elements that leads the plain's susceptibility to flooding.

A comprehensive understanding of the historical context of flood and flood pattern in the Upper Nile plain requires a reconstruction of historical climatic conditions and thorough investigation of the factors contributing to the plain's susceptibility to flooding. However, due to limited historical data, most of the attempts made by researchers to understanding climatic conditions that contributed to flooding in the past were based on inference derived from recorded condition in adjoining territories (Johnson, 1992).

Flood occurrence in the Upper Nile plain and thus Upper Nile state, and the pattern of flooding in general can be ascribe to multitude of factors within the plain and in adjacent regions. Johnson (2019) has noted this, pointing out that the occurrence of flood is less dependent on local rainfall than on rainfall in other parts of northeast Africa. Precipitation regimes in Ethiopian highlands, East African lakes and East Equatorian mountains, coupling with local rains lead to episodic variations in the Sobat River system and the Nile's discharge. These changes, adding to it the flat topography and impermeable clay soil of the plain, along with the poorly defined and low banks of the Bahr al-Jabal that connect at Bahr al-Ghazal to form the White Nile, spills easily into the Sudd Swamp where vegetation blockage hinders flow and redirect it into shifting channels, thereby influences the occurrence and pattern of floods within the Upper Nile plain and thus the study area. During wet season (May - October), a period of high Nile discharge and heavy rainfall leads to pluvial and fluvial flooding. "River flooding combines with rain flooding (standing water on the clay plain) and in years of exceptionally high rivers and heavy rains there can be the added hazard of a 'creeping flood'[...]." (Johnson, 1986, p. 133;134)

2.2.2. History Of Floods: A Geohistorical and Anthropological Perspective

Records of flood occurrences found in historical documents, anthropological commentaries and related literature for Upper Nile plain (Lyons, 1907; Hurst, 1920; J. I. Team, 1953; S. D. I. Team, 1954; Johnson, 1986, 1989, 1992; Hassan, 2007) provides extensive and systematic details of flood dating back as far the 18th century. These records were derived from oral testimonies, Egyptian Nile records, local administrative reports, and more recent methodical measurement of the Nile's discharge inside Sudan, initiated in the late twentieth century. These documented records are indispensable source of information concerning extreme climatic events such as floods and drought in the Upper Nile plain. However, it is imperative to also acknowledge that, since these literary sources encompass the entire Upper Nile plain which relatively corresponds to present-day Upper Nile region, presents a challenge in precisely determining the geographical context of historical and anthropological records of flood for the designated research area (Upper Nile state). Therefore, the brief accounts derived from these literary sources and presented here are only tentative and concentrated solely on incidence of flooding along Bahr al-Zaraf, the Sobat River and the White Nile, hypothesised to have exerted influence on the research area. A brief account on major flooding from the nineteenth century up to date is provided below the descriptive Table 2.

Period	Time scale	Local names of flood	Meaning
19th Century	1820 - 1830	Amol Magook	Flood of *Magook*
	1878 - 1880	Nyoc Bor	The White flood
20th Century	1916 - 1917	Pibor	The white water
	1917 - 1919	Pilual	The red water
	1962 - 1970	Nyotch	The year of big flood
	2017 - 2018	Luwar	The year of small flood
21st Century	2018 - 2019	Luwar	The year of small flood
	2019 - 2020	Luwar	The year of small flood
	2020 - 2021	Nyotch	The year of big flood
	2021 - 2022	Ruonjiek	The year of the worst flood

Table 2. Chronological order of major historical flood events

2.2.2.1. The period between 1800 -1900

This period as most of the historical documents and related literature suggest, is known for the occurrence of two major floods, *Amol Magook* and *Nyoc Bor*. Inhabitants residing near *Khor Atar and Fulluth,* watercourses adjacent to the White Nile River recalled a major flood that happened during the rule of the Shilluk monarch (1820 – 1830) Akwot Nyakwac (Johnson, 1992). This flood referred to as *Amol Magook*, denoted in the memory of tribal man named *Magook* who tragically perished is known to have originated from the eastern direction, the Sobat River. Hence, this implies a period of above average rainfall in Ethiopian region, which in turn led to the inundation of the Sobat River. The impact of the flood was severe, resulting

into extensive destruction of agricultural yields, grazing lands, livestock, human livelihood, and triggering emigration of the surviving population to higher grounds – *Duk Ridge*. As illustrated in Table 2, perhaps the most severe of all the flooding event that took place in the 19the century occurred in the year 1878. During this period in time, the Upper Nile plains was hit by a flood that, in term of magnitude, surpassed the flood that began in 1820 (Amol Magook). This flood has come to be known as *Nyoc Bor* meaning *the white flood*. The name was later changed to *Nyoc Bor Mogogh* donating a famous battle that took place right after the flood. "The flood of 1878, though tremendous, dropped quickly and had no lasting effect on the *Nuer* settlement" (Johnson, 2019, p. 185). The following decade (1880 – 1890), although characterised by decline in the water level of Lake Victoria, due to severe blockage in the *Sudd* swamp, there were still series of small floods affecting the plains.

2.2.2.2. The Period Between 1900 – 2000

During the first half of the twentieth century, notably the period from 1916 to 1919 as indicated in Table 2, the Upper Nile flood plain experienced another severe flooding of unparalleled magnitude. Two waves of floods – called *Pibor* and *Pilual* – began on the October of 1916 and persisted for a duration of eighteen months, submerging entire districts from *Bor* to *Malakal* and extending from *Kongor* to *Pibor river*. These waves of floods were caused by the combination of two factors: the prevailing hydrological and climatic conditions at that time. Hurts' (1920) observations shows that, the rise in the level of East African lakes including Lake Victoria that began a year prior to the floods and maintained a consistent high state until 1918, heavy precipitation in Ethiopian regions that raised the level of Sobat river to the highest ever recorded level, along with intense local rainfalls, substantially contributed to the level of standing water and leading to 'creeping flood'. The first wave of flood, referred to as *Pibor* was observed to be approaching from western direction. And although the first wave exhibited a less destructive impact, before water could fully recede, a second wave of flood – *Pilual* (the red water) – came, exacerbating the effects of the first flood. The entire Area between Bahr al-Zaraf and Duk ridge was submerge for two years, causing mass movement of local communities to higher grounds. There was a wide spread of rinderpest and other cattle disease especially in the area along *Fangak* – southwestern border of the study area. According to Johnson (Johnson, 1989), *Pibor* and *Pilual* were understood to be the most disastrous of all the floods the occurred in the first half of the twentieth century in the entire Upper Nile Region. Furthermore, Oral accounts from participants in a focus group discussions carried out

in line with shock verification mission for Fangak county[7], a county in the lower reaches of the White Nile shows that, the second half of the twentieth century (period between 1962 – 1970) had witnessed the longest ever recorded period of inundation. Named locally as *Nyotch* (a year of the big flood), this flood was marked by extensive inundation and higher level of damages (Table 2), comparable in magnitude only to the recent flood of 2021.

2.2.2.3. Recent Flood Events

Seasonal flooding is a recognized naturally occurring disaster in the Upper Nile state. In the past, there have been structural measures and adaptation strategies to minimize the impact of flood hazards (i.e., construction of dykes, channelisation, seasonal emigration, the development of livelihoods base on 'common economy'[8], and the like). In recent years however, (despite the measures in place or therefore, lack of) the gradual increase in both the frequency and extent of flood phenomenon which to some extent resembles the deleterious flood of 1962, and the existing social and political conflict which Tiitmamer et al. (2018) suggested could have been exacerbated by climate change since conflicts occurs after the occurrence of environmental disasters in itself, have strongly affected the resilience of local communities.

The wave of seasonal flooding in the last decade that began in 2017, had primarily impacted Maban county in the eastern part of the study area. The inundation resulted in displacement of hundreds of people, and extensive damage to road infrastructure and farmlands causing food insecurity. Subsequently, the flood experienced in 2017, as well as in the ensuing years namely the flood of 2018 and 2019 which affected several counties in the southeastern part of the study area (Maban, Longochuk, Maiwut, Nasir, and Ulang) with Maban being affect the most, earned the local name 'years of small flood'. This name is mainly attributed to the extend and magnitude of these floods which closely aligned with local precipitation pattern. Notably these flood events, are caused by torrential rains in wet seasons and exhibited a relatively rapid recession during the dry seasons. In 2020, however, before a complete recession of waters from previous year's flood, heavy rains caused rivers to breach dykes and banks, leading to protracted period of inundation of vast areas and settlements.

---

[7] ACTED & REACH. (2021) "Fangak Shocking Verification Mission: Jonglei State, South Sudan, June 2021" https://reliefweb.int/organization/reach-0

[8] 'Common economy' is a form of social and economic network that was identified by Evans-Pritchard while investigating the mode of livelihood and political institution of the Nilotic people. This type of social and economic network which in its essence is applied during times of environmental disasters such as floods, is a survival strategy that relies on common consumption and reciprocal assistance between larger communities, guided by factors such as familial ties, affinity and membership within specific age group (Evans-Pritchard, 1940).

About 30,000 people were reported to have been impacted in Renk county – northern part of the study area (ECHO, 2020). Official from World Food Programme (WFP) characterised this flooding as potentially the most severe in six decades (Mayen et al., 2022). Certain aspects of the 2020 – 2021 flooding, such as elevated water levels and unusually accelerated water flow, surpassed the severity observed during the 1962 flood event. The recurrent flood pattern, stemming from substantial rainfall during wet seasons in both downstream and upstream, coupled with the prolonged presence of floodwater from prior years, endured throughout 2021 and 2022. In the year 2021, vast areas in the Upper Nile state experienced two instances of inundation and this has placed considerable strain on local coping mechanisms, affecting more than 50,000 individuals across three counties in Upper Nile state, namely Ulang, Fashoda, and Longechuk county (IRNA,2021).

3. DATA ACQUISTATION AND ANALYSIS METHODS

3.1. Criteria identification and data sources

This study is based on the application of multi-criteria decision analysis and the analytical hierarchy process in flood hazard mapping. The initial phase in the research involves the identification of flood influencing factors; these are, meteorological and physical characteristics of the study area which to enhance the area's susceptibility to flooding. The successful application of the MCDA-AHP method to identify flood-prone areas is highly contingent upon the recognition of these factors and their inter-relation with the mechanisms contributing to flood occurrence. Moreover, these factors serves as the criteria within the MCDA model applied for analysing areas susceptible to flood (Mudashiru et al., 2021).

Data source	Resolution / scale	Dates	Role / Function	Citation
Rivers of Sudan - AFRICOVER	1: 250 000	Vector data: 2003-05-30	River network	www.data.apps.fao.org
Shuttle Radar Topography Mission (SRTM)digital elevation model (DEM)	30 metres	31 images: 2014-09-23	Topographic wetness index; drainage density; slope; elevation	NASA (2013)
ESA Sentinel – 2 10m land uses/ land cover time-series layer	10 metres	4 images: 2021-01-01	Land use / land cover	Karra et al. (2021)
Climate Research Unit (CRU) TS v4.06 Annual mean rainfall 2010-2021	0.5°x 0.5°	2022-05-26	Annual average rainfall (2010-2021)	Harris et al. (2020)
The digital soil map of the world	1:5.000.000	Vector data: 2003-01-01	Soil types	FA0 (1974)
Visible Infrared Imaging Radiometer Suite (VIIRS)	375 metres	Images: 2020-10-19 2021-10-19 2022-10-21	Inundation extent map	www.ladsweb.modaps.eosdis.nasa.gov

Table 3. Conventional (vector) and remote sensing (raster) data sources.

Numerous studies have used a wide range of flood influencing factors in delineating flood hazard zones. Although there is no uniformity regarding the selection of these factors and their relative importance as Allafta and Opp (2021) pointed out, researchers often determine their selections either on the literature or the physical and natural characteristics of the area under investigation or sometimes both. In the current study, drawing upon existing literature as foundational basis (Danso et al., 2020; Ogato et al., 2020; Ajibade et al., 2021) and the physical

characteristic of the study area, eight flood influencing factors have been chosen: namely, (1) distance to the river, (2) topographic wetness index, (3) drainage density, (4) land coverage, (5) precipitation, (6) slope, (7) elevation, and (8) soil type. Raster and vector datasets for the selected factors were obtained from different web sources, re-projected, analysed, and subsequently reclassified into standardised form in ArcGIS Pro (Figure 3). This preparatory phase holds a considerable importance as it enables the overlay analysis resulting in the generation of the flood hazard index.

The distance to the river layer was derived from Sudan's primary rivers vector dataset produced by the Food and Agriculture Organisation (Table 3). Using 'Distance Accumulation' function in 'Spatial Analyst Tools', distances to the major perennial rivers; namely, White Nile, the Sobat and its tributaries within the study area (river Pibor and Baro), Doleib, Bibban, El-Samaa, Wehfet, Adar, Yale, Tombak, Yabus, Daga, and river Nyanding were measured and subsequently classified into five classes based on the distance range. Topographic wetness index (TWI) layer was obtained from the Shuttler Radar Topography Misson (SRTM) Digital Elevation Model (Table 3). 'Hydrology' and 'Map Algebra' functions in 'Spatial Analyst Tools' were applied to combine the catchment and slope of the study area, which yielded an index that describes the propensity of water accumulation in the study area. Furthermore, and using the same SRTM digital elevation model, layers depicting drainage density, slope, and elevation properties of the study area were generated. The generated additional three layers were reclassified into a standardised in same cell size as the prior two layers. The land-coverage layer on the other hand, was obtained from Esri's global land use/ landcover data (Table 3). The downloaded scenes – 35N, 35P, 36N, 36P – were mosaicked into one raster dataset, and each land use/land cover class was relabelled and reclassified accordingly. For computation of the annual average rainfall layer, rainfall data for the period between 2020 to 2021 was retrieved from the Climate Research Unit database (www.uea.ac.uk). Essentially, the Climatic Research Unit gridded Time Series (CRU TS) climate dataset is generated through the interpolation of monthly climate anomalies extrapolated from comprehensive networks of weather station observations around the globe (Harris et al., 2020). In the study area, two weather stations that actively collected rainfall data – Renk and Malakal weather stations (Figure 4). The obtained data from the Climate Research Unit was transformed into raster layer using 'Multidimensional Tools' and 'Make NetCDF Raster Layer', and subsequently converted to points using 'Conversion Tools', 'From Raster' and 'Raster to Points'. The points were interpolated using 'Kriging' function in 'Spatial Analysts Tools' generating annual average

rainfall layer. This layer was further reclassified using equal interval classification method in ArcGIS Pro into a map with five classes. Lastly, the soil type map was obtained from the Food and Agriculture Organisation digital soil map of the world (www.livingatlas.arcgis.com). The soil type data for the study area was extracted from the digital soil map of the world using 'Pairwise Clip' function in 'Analysis Tools'. The Attained layer was reprojected, and each soil type was geo-coded to the lithology of the study area. Subsequently, the polygon soil layer was transformed into raster using 'Conversion Tools' and 'Polygon to Raster' and reclassified into standardised format.
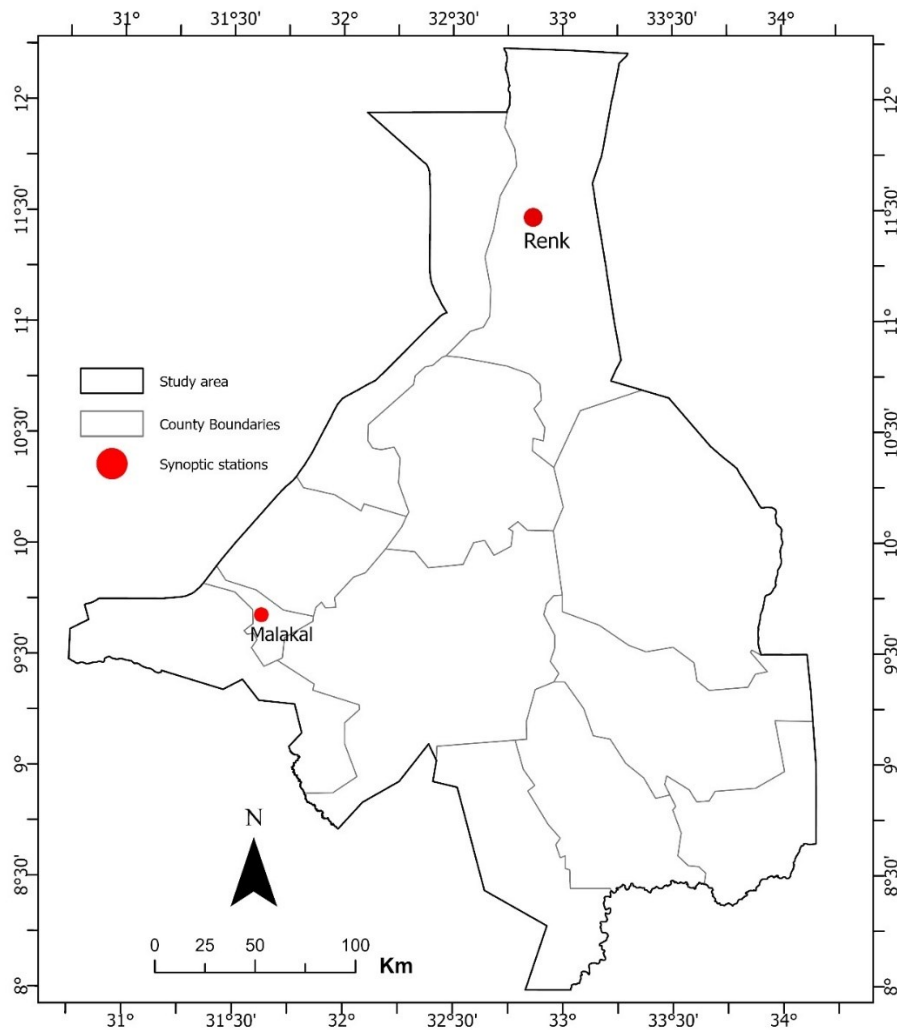
Figure 4. Location map of meteorological stations within the study area.

3.3.1. Flood Influencing Factors

3.1.1.1. Distance to rivers

Proximity to perennial water bodies such as rivers and stream exerts a great degree of effect on the spatial distribution of flood occurrence. As evidenced in the existing literature, the

incidence of flood disaster is closely linked to the river distribution network (Allafta & Opp, 2021). Moreover, the extent and intensity of a flood, particularly in the case of pluvial flood, is more severe in areas close to perennial water bodies (Glenn et al., 2012). As distance to river diminishes, a region's exposure to flood events increases, hence acknowledging the influence of river proximity and including it as a factor within flood hazard model holds a considerable significance. Numerous studies examining flood hazard susceptibility using the multi-criteria decision method have integrated distance to the river as one of the key factors, assigning a high weight as evidenced in Kazakis et al. (2015); Khaleghi & Mahmoodi, (2017). In this study, distance to the river was used as one of the evaluated flood influencing factors with a relative weight determined by experts.

3.1.1.2. Topographic Wetness Index

Topographic Wetness Index (TWI) assesses the effect of topographical characteristics on the degree of soil wetness and how slope affects hydrological processes. It "describes water accumulation trend at a particular location, and the local slope shows the influence of gravitational forces on the water flow" (Parsian et al., 2021, p. 8). Computation of TWI is based on two factors; these are, slope and elevation of the terrain. An elevated value of TWI signifies high level of surface moisture, whereas a low value indicates a dry surface. TWI have a wide range of applications, such as modelling hydrological and biological processes, vegetation patterns, flooding modelling, and mapping areas susceptible to flood. The application of TWI in flood hazard mapping can be achieved using two distinct approaches. On one hand, TWI can be employed as a sole tool in delineating flood-prone areas, as demonstrated in Pourali et al. (2016); Kelleher & McPhillips (2020); and Saputra et al. (2023), on the other hand, it can be integrated with other relevant parameters within one model to generate flood hazard index (Fernández & Lutz, 2010; Arabameri et al., 2019). In the current study, the slope and Digital Elevation model were used to calculate Topographic wetness index of the study area using equation (1).

(1)
$$\text{TWI} = In\left(\frac{SCA}{tan\beta}\right)$$

Where *SCA* donates specific catchment area which is an in integration of surface and subsurface drainage per unit contour width – equation (2), and *tanβ* is percent slope.

(2)
$$\text{SCA} = \left(\frac{catchment\ area(m^2)}{unit\ contour\ width}\right)$$

3.1.1.3 Drainage density

Generally, drainage density is a measurement that assesses the capacity of stream channels to drain a catchment (Horton, 1945). Defined as the cumulative length of all stream networks divided by catchment area, a drainage density of a catchment affects the temporal dynamics and concentration of surface runoff, and this has implications in the spatial distribution of flood. An elevated drainage density leads to high volume of water transportation downstream. Consequently, yielding an earlier culmination of peak flow in response to rainfall. This, in turn, exert a proportional influence on the extent and duration of flood disaster. In the current study, drainage density was used a s proportional criterion and calculated using equation (3). The study area is comprised of 24 basins of varying sizes. The most diminutive basin encompasses an area of 2 kilometres square, whereas the largest basin covers an area of 11,667 kilometres square (Figure 5).

$$\mathrm{D_d} = \frac{\Sigma L}{A}$$
(3)

Where D_d = drainage density; ΣL = total stream length of all order; A = the study area

3.1.1.4. Land-coverage (Land uses/land cover)

Various categories of land-coverage exert varying effect on both infiltration rates and debris flow (Kazakis et al., 2015). The impact of land-coverage on the intricate relationship between surface and ground water has significant implication for the occurrence of flood events. For instance, while bare land favours surface water runoff, an area with thick vegetation cover supports infiltration. The presence of substantial vegetation cover improves surface roughness which has the effect of diminishing surface water runoff and increasing infiltration rate. Impervious surfaces like buildings and surfaces that have been inundated for long period of time on the other hand, exhibit an almost negligible capacity to absorb water, consequently elevating the volume of water runoff. As such, an area with dense vegetation exhibits relatively low vulnerability to flood incidents due to high infiltration rate, whereas urban and pasture areas are more exposed to flood incidents due to low infiltration rate and high surface runoff in response to rainfall. Considering this aspect, the land use/land cover classes of the study area were integrated into the flood hazard model. The rank of each land use/land cover class within the model was based their influence on filtration rate and surface water runoff.
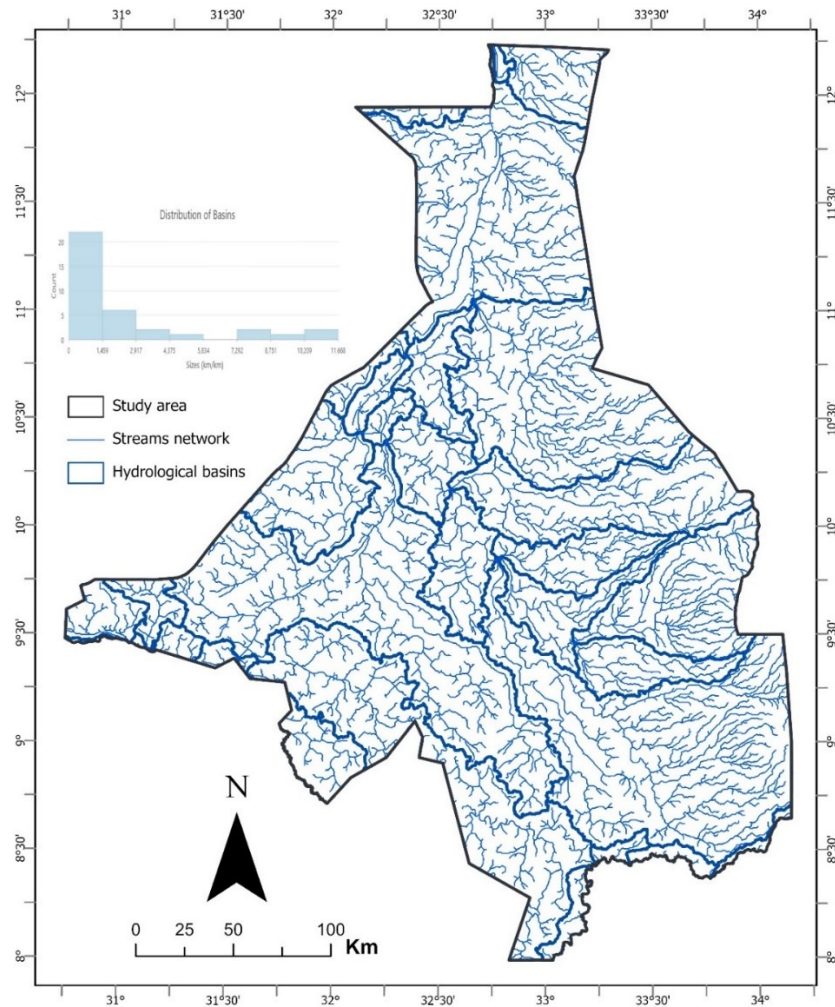
Figure 5. Distribution of hydrological basins and hydrography in the study area.

3.1.1.5. Rainfall

Rainfall plays a major role in the evolution of flood hazards, and it is the most and critical trigger of flood disasters (L. Liu et al., 2022). Increase in the intensity, frequency, and duration of rainfall, coupled with topographical and hydrological characteristics of a region, can augment that region's vulnerability to flood events. A sudden intense rainfall that persists for a long period of time has the potential to exhaust the natural drainage system within a region, consequently influencing the volume of discharge into rivers and streams. This, in turn, may surpass the carrying capacity of stream and river networks in a region, resulting into overflow of rivers and ultimately flood events. As such, the assessment of a region's vulnerability to flood hazards, particularly in the case of flash flood hinges significantly on the consideration of rainfall patterns. Numerous research endeavours focused on examining flood-prone areas predominantly incorporated this factor as a crucial evaluation criterion (see: Kazakis et al., 2015; L. Liu et al., 2022; Vaddiraju & Talari, 2022; Bagyaraj et al., 2023). In contrast to the

34

prevalent use of monthly average rainfall periods, predominantly considered in flood frequency analysis, the present study adopts an annual average rainfall dataset spanning the period from 2010 to 2021. This is mainly due to the study's objective to delineate the probabilistic geographic extent of a flood hazard, taking in to account the influence of the pattern of annual rainfall periods on the evolution of flood hazards.

3.1.1.6. Digital Elevation Model (DEM)

Elevation represents a crucial parameter widely use in studies evaluating flood hazards. Low-lying areas are more exposed to water overflow originating from steep, elevated terrains, rendering them more susceptible to accumulation of flood waters as opposed to areas characterised by higher elevation. "Water flows from higher to lower elevations and therefore slope influences the amount of surface runoff and infiltration; [and] flat areas in low elevation may flood quicker than areas in higher elevation with a steeper slope" (Kazakis et al., 2015, p. 4). Consequently, the elevation of an area plays a pivotal role as a determinant factor in assessing its vulnerability to flood hazards. Data depicting the absolute elevation of study area was used among the criteria to identify areas with an increased susceptibility to water accumulation within the flood hazard model.

3.1.1.7. Slope

The occurrence of flood is closely linked to the slope of terrain, primarily influence by the speed at which surface runoff travels and accumulates downstream. Hence, slope gradient and elevation of an area are interrelated factors that jointly shape the spatial distribution of floods. For instance, in an area with high elevation and steep slope, water flows at a high speed therefore reducing the possibility of standing water. This surface runoff from highlands, however, accumulates downstream in flat areas with low elevation resulting into difference in the spatial distribution of flooding. The steeper the slope of terrain is, the potential of flood occurrence diminishes, whereas the lower the slope, the proneness of area to flood hazard increases (Wu et al., 2015).

3.1.1.8. Soil type

The major role of soil in flood occurrence is inherently related the type of a soil and the capacity of soil to retain water. Different soil types exhibit varying degree of infiltration capacity which can remarkably influence the volume of standing water. Intense rainfall in general results in faster and greater runoff in clay and loam soils in comparison to sandy soil. Hence accounting for soil types and their effect on infiltration rate and surface runoff is crucial in delineating flood hazard zones.
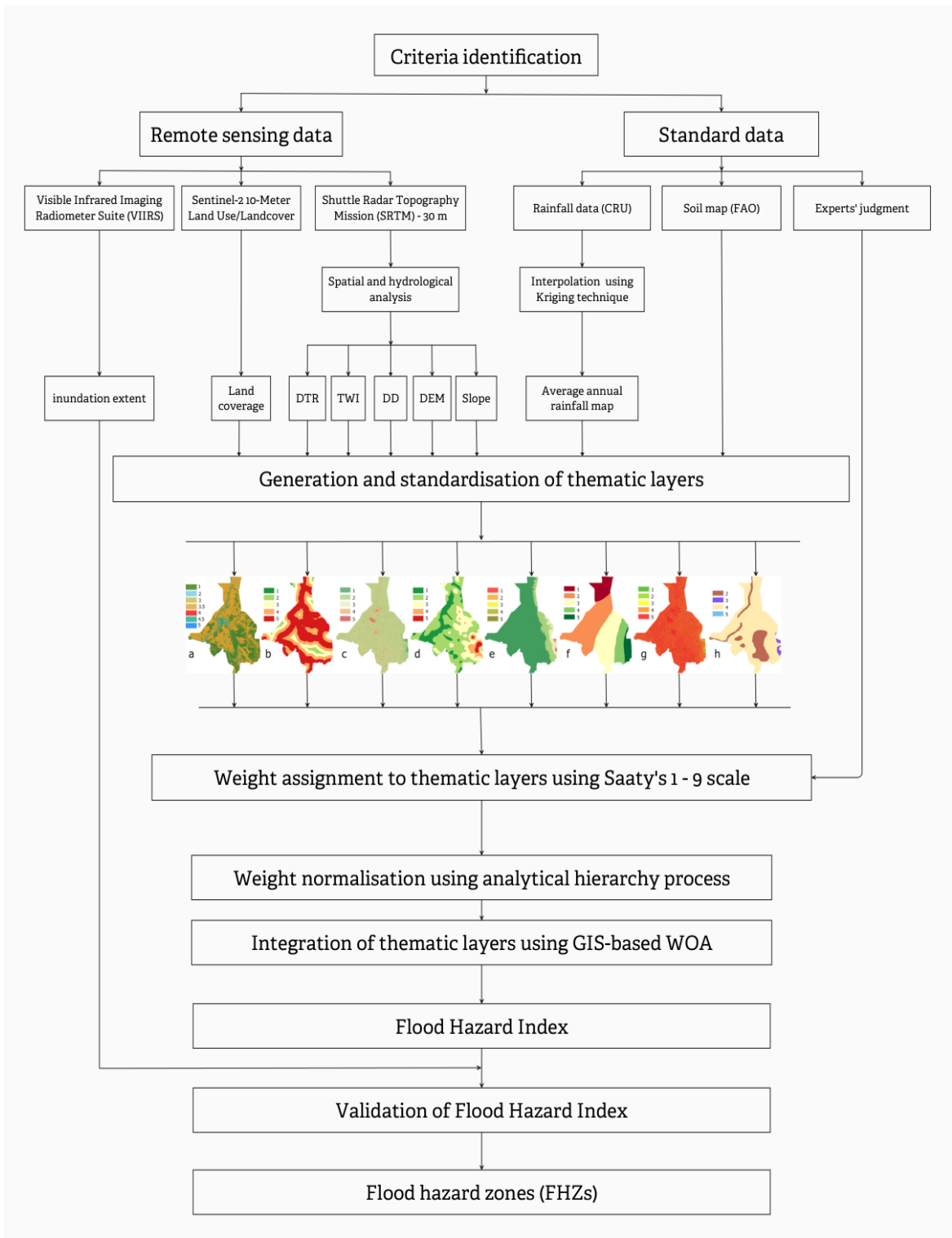
Figure 6. Flowchart of the adopted methodology for flood hazard susceptibility mapping. Note: DTR = Distance to the river; TWI = Topographic wetness index; DD = Drainage density; DEM = Digital elevation model; WOA = Weighted overlay analysis.

3.2. Analytical hierarchy process

Following the preliminary stage of generating and standardising thematic layers, the analytical hierarchy process was applied to assign *weights*[9] to each flood influencing factor based on its relative significance in the evolution of flood hazards. The analytical hierarchy process is a semi-quantitative methodology that facilitates the estimation of criteria weights by drawing upon experts' opinions regarding the relative significance of each criterion (Dash & Sar, 2020). In this context, the development of the weights to determine the relevance of each criteria in the process of delineating areas susceptible to flood hazard was therefore, accomplished using Saaty's (1990) 1 – 9 scale (Table 4). A structured questionnaire was sent to 15 professional encompassing experts in climatology, geomorphology, Hydrology, urban planning, and GIS analysis. The objective was to collect their judgement regarding the weight of each criteria. Among the 15 experts, eight experts actively participated by providing their considered judgments and opinions. The questionnaire table was made up of eight weight flood influencing factors (distance to the river, Topographic Wetness Index, drainage density, land-coverage, rainfall, slope, Digital elevation Model, and soil type). Each expert was asked to compare each criterion against another criterion and assigned to it a value based on its level of importance on flood occurrence using Saaty's (1990) 1 -9 scale.

Level of importance	Definition	Explanation
1	Equal Importance	Two activities contribute equally to the objective
3	Moderate Importance of one over the other	Slight preference for one activity based experience and judgment
5	Essential or strong importance	Significant preference for one activity based experience and judgment
7	Very strong importance	An activity is strongly favoured, and its dominance is demonstrated in practice
9	Extreme importance	The evidence of favouring one activity over another is of the highest order of affirmation
2,4,6,8	Intermediate values between the two adjacent judgments	Used when compromise is need

Table 4. 1- 9 scale of importance (T. L. Saaty, 1989, 1990)

3.3.1. Aggregation of Experts' Judgements and the Pairwise Comparison Matrix

The ratings obtained from the survey with the experts were incorporated in an AHP Excel Spreadsheet established by Goepel (2013). Within this excel spreadsheet, a pairwise

---

[9] "A weight can be defined as a value assigned to an evaluation criterion indicative of its importance relative to other criteria under consideration" (Drobne & Lisec, 2009).

comparison matrix was formulated for every expert, expressing their individual judgement. Subsequently, the principal eigenvector and corresponding eigenvalue for each decision matrix was computed, and the consistency ratio of each was determined. This process facilitates the derivation of priority vector for each expert. The priority vectors, derived for each of the expert participating in this study, were then aggregated using weighted geometric mean to construct a consolidate pairwise comparison matrix expressing the collective judgement of the experts (Table 5).

To normalise the consolidate pairwise comparison matrix score, each entry in the column of the matrix was divided by its column sum using equation (4), yielding a normalised pairwise comparison Matrix with the sum of 1 for each column in the matrix (Table 6) – equation (4).

(4) $$W = (w_1, w_2, \ldots, w_j, w_n), \text{ and } \sum w_j = 1$$

The sum of the normalised score for each row was divided by the number of criteria, yielding an average score for elements in each row. These computed averages offer an approximation of the relative weights of the relevant criteria as illustrated in Table 7 (Drobne & Lisec, 2009).

(5) $$w_n = \left(GM_n \Big/ \sum_{n=1}^{ni} GM_n \right)$$

Criteria	Distance to river	Topographic Wetness Index	Drainage density	Land-coverage	Rainfall	Slope	Digital Elevation Model	Soil type
Distance to rivers		1.08	1.17	1.78	1.26	1.63	3.6	4.26
Topographic Wetness Index	0.93		1.14	1.37	1.74	1.66	1.72	2.89
Drainage density	0.85	0.88		0.82	1.3	1.54	2.33	2.97
Land-coverage	0.56	0.73	1.21		1.54	1.46	1.74	2.3
Rainfall	0.79	0.57	0.77	0.65		1.39	1.94	3.6
Slope	0.62	0.6	0.65	0.69	0.72		3.39	2.76
Digital Elevation Model	0.28	0.58	0.43	0.57	0.51	0.3		2.02
Soil type	0.23	0.35	0.34	0.43	0.28	0.36	0.5	

Table 5. Consolidated geometric weighted means of the expert's judgement.

Criteria	Distance to the river	Topographic Wetness Index	Drainage density	Land-coverage	Rainfall	Slope	Digital Elevation Model	Soil type
Distance to rivers	0.19	0.19	0.17	0.24	0.15	0.17	0.22	0.20
Topographic Wetness Index	0.18	0.17	0.17	0.19	0.21	0.18	0.11	0.13
Drainage density	0.16	0.15	0.15	0.11	0.16	0.17	0.14	0.14
Land-coverage	0.11	0.13	0.18	0.14	0.18	0.16	0.11	0.11
Rainfall	0.15	0.10	0.11	0.09	0.12	0.15	0.12	0.17
Slope	0.12	0.10	0.10	0.09	0.09	0.11	0.21	0.13
Digital Elevation Model	0.05	0.10	0.06	0.08	0.06	0.03	0.06	0.09
Soil type	0.04	0.06	0.05	0.06	0.03	0.04	0.03	0.05
Sum	**1**	**1**	**1**	**1**	**1**	**1**	**1**	**1**

Table 6. Normalised pairwise comparison matrix of flood influencing factors (Criteria).

Criteria	Non-normalised values (EVM)	Error +/-	Normalised values (EVM)	Influence (%)
Distance to rivers	0.192	0.031	0.19	19.19%
Topographic Wetness Index	0.166	0.033	0.17	16.63%
Drainage density	0.147	0.020	0.15	14.73%
Land-coverage	0.138	0.035	0.14	13.83%
Rainfall	0.126	0.028	0.13	12.61%
Slope	0.118	0.044	0.12	11.81%
Digital Elevation Model	0.067	0.020	0.07	6.71%
Soil type	0.045	0.009	0.04	4.49%
Sum	**1**	**0.219**	**1**	100.00%

Table 7. Non-normalised and Normalised principal Eigenvector weights of each flood influencing factor.

3.2.2. Matrix Consistency

After creating the eigenvector for the analytical hierarchy process pairwise matrix which contains the relative weight of each criterion, it is crucial to assess the consistency ratio of the matrix. This necessity arises due to the fact that the computed averages only provide an estimate of the relative weights of the relevant criteria. These weights, construed as the average outcomes across all conceivable pairwise comparisons of criteria, denote the aggregate preferences of experts. Given that the complete ratio matrix encompasses multiple paths through which the relative significance of criteria can be assessed, it is significant to examine whether the path determined by experts manifests coherence and validity in the context of the decision problem under consideration (Drobne & Lisec, 2009).

The consistency ratio quantifies the likelihood that a matrix scorings were generated randomly, and a matrix consistency is established only when the consistency ratio falls within the range of less than or equal to 0.1. In cases where the consistency ratio exceeds 0.1, it is imperative to re-evaluated the initial scoring of the matrix (Saaty, 1990).

In order to compute the consistency ratio, the initial procedure involves the calculation of the principal eigenvalue (λ_{max}). The principal eigenvalue (λ_{max}), is used to measure the degree to which the matrix deviates from state of consistency. A principal of eigenvalue equal to or greater than the total number of evaluated criteria signifies the matrix's consistency, thus enabling the computation of consistency ratio. Conversely, a principal eigenvalue (λ_{max}) that is less than the total number of evaluated criteria signals inconsistency in the matrix, thus indicating the need for re-evaluation of the initial pairwise matrix (Saaty, 1977;Saaty & Vargas, 2012).

Criteria	Sum of Pairwise decimal matrix Table 5 (A)	Normalised weight Table 7 (B)	Criteria Rank (A)*(B)
Distance to rivers	5.27	0.19	1.01
Topographic Wetness Index	5.79	0.17	0.96
Drainage density	6.71	0.15	0.99
Land-coverage	7.31	0.14	1.01
Rainfall	8.36	0.13	1.05
Slope	9.34	0.12	1.10
Digital Elevation Model	16.23	0.07	1.09
Soil type	21.79	0.04	0.98
Sum (λ_{max})			**8.20**

Table 8. Computation of the principal Eigenvalue (λ_{max}) to determine the influence of each criterion.

To determine the principal eigenvalue (λ_{max}), the weight of the first criterion was multiplied by the sum of the first column of the original pairwise. A similar procedure was applied to the second criterion, where its weight was multiplied by the sum of the values in the second column, and so forth, for all the criteria. Upon executing this procedure for each criterion, a principal eigenvalue of **8.20** was derived from a matrix of **8*8** (Table 8), which exceeds the number of evaluated criteria, and therefore, was deemed acceptable. Subsequently, the principal eigenvalue was used to compute the consistency ratio of the pairwise matrix.

No.	Random Indices	No.	Random Indices	No.	Random Indices
1	0.00	6	1.24	11	1.51
2	0.00	7	1.32	12	1.54
3	0.58	8	1.41	13	1.56
4	0.90	9	1.45	14	1.57
5	1.12	10	1.49	15	1.59

Table 9. Random Indices for varying set of criteria (Saaty, 1977)

A consistency ratio is the division of the consistency index by Random Index, denoted as:

(6) $$\mathrm{CR} = \frac{CI}{RI}$$

Where *RI* is a *Random Index* and *CI is a Consistency Index.* On the one hand, a Random Index signifies the consistency index of the pairwise comparison matrix that is generated randomly and its value is contingent upon the number of criteria under evaluation. Different Random Indices for different number of criteria is presented in Table 9. Since the study evaluated 8 different criteria, the standard Random Index for the evaluated criteria is **1.41.** Consistency Index on the other hand, provides a measure of departure from consistency based on the principal eigenvalue; denoted as (7).

(7) $$\mathrm{CI} = \frac{\lambda_{max} - n_i}{n_1 - 1}$$

The Consistency Index of the matrix equates to 0.029 as shown in computation *8*, and the Consistency Ratio is determined to be 2.0 % as indicated in computation *9*. Hence, given that

the Consistency ratio is 2.0 %, a value lower than the recommended threshold of 10 % as proposed by (Saaty, 1977), it is deemed appropriate to proceed with the overlay analysis to derive the flood hazard index and produced flood hazard susceptibility map for the study area.

$$(8) \qquad \text{CI} \ = \frac{8.20 - 8}{8 - 1} = 0.029$$

$$(9) \qquad \text{CR} \ = \frac{0.029}{1.41} = 0.020 = 2.0 \ \%$$

3.3. Weighted overlay analysis and flood hazard index

3.3.1. Classification of Thematic Layers

The underlying assumption with the linear combination method is that each factor has an interval range which are clustered on a ratio scale. As such the value range of thematic raster layers used in this study were each normalised on a scale of 1 to 5. The classes for the value range of the thematic layers were established using different approaches, including equal intervals, natural breaks, and lithological units among others, with the aim of enhancing objectivity (Dash & Sar, 2020). The selection of these methods was driven by two specific objectives: (1) first to ensure that the variance with each class is minimised to an acceptable threshold, while the variance between classes is maximised; (2) and secondly, to ensure a classification scheme that aligned with, and takes into account the inherent physical characteristics of the study area and the pattern of flooding occurrence.

Quantitative criteria were clustered into categories through the application of two distinct classification method. Equal intervals were applied to group criteria such as distance to rivers, drainage density, and annual average rainfall. In contrast, natural were utilised for criteria such as Topographic Wetness index, slope, and DEM. This approach allowed for a tailored and effective classification strategy based on the specific nature of each criterion. While the equal interval method produces an equal class width with varying frequency of observation, the natural break method account for non-uniform distributions, giving an unequal class width with varying frequency of observation per class.

Qualitative criteria on the other hand, were grouped according to the specific local topographical characteristics of the study area. The classification of soil types was contingent upon the prevailing properties of the predominant soil types that makes up the terrain of the study area. Additionally, the categorisation of land-coverage was determined by employing

Esri's detailed land use/ landcover classes, which were derived through the utilisation of artificial intelligence model (www.livingatlas.arcgis.com).

Considering the influence of each criterion in flooding, the pixels within each criterion were assigned values ranging from one (minimum influence in flood occurrence) to 5 (maximum influence in flood occurrence).

Criteria	Unit	Classification method	Class width	Flood hazard influence	Criteria weight (%)	Rank
Distances to rivers	Metres	Equal interval	≤ 14,000	Very high	19.19 %	5
			14,000 - 28,000	High		4
			28,000 - 42,000	Moderate		3
			42,000 - 56,000	Low		3
			≥ 56,000	Very Low		1
Topographic Wetness Index	Level	Natural breaks	≤ 12.5	Very low	16.63 %	1
			12.5 - 14.5	low		2
			14.5 - 16. 5	moderate		3
			16.5 - 18.5	high		4
			≥ 18.5	Very high		5
Drainage Density	Km/Km^2	Equal interval	≤ 0.60	Very Low	14.73 %	5
			0.60 - 0.90	Low		4
			0.90 - 1.20	Moderate		3
			1.20 - 1.50	High		2
			≥ 1.50	Very high		1
Land-coverage (LULC)	Type	AI based unsupervised classification	Dense vegetation	Extremely low	13.83 %	1
			Crop land	Very low		2
			Bare land	Low		3
			Pastureland	Moderate		3.5
			Built area	High		4
			Flooded vegetation	Very High		4.5
			Water	Extremely high		5
Rainfall	Mm/yr.	Equal interval	≤ 680	Very low	12.61 %	1
			680 - 810	Low		2
			810 - 940	Moderate		3
			940 - 1070	High		4
			≥ 1070	Very high		5
Slope	Degree	Natural breaks	≤ 1	Very high	11.81 %	5
			1 - 6	High		4
			6 - 11	Moderate		3
			11- 22	Low		2
			≥ 22	Very Low		1
Digital Elevation Model	Metres	Natural breaks	≤ 420	Very high	6.71 %	5
			420 - 480	High		4
			480 - 640	Moderate		3
			640 - 970	Low		2
			≥ 970	Very low		1
Soil type	Type	Lithological unit	water	Very High	4.49 %	5
			clay	High		4
			Clay loam	Moderate		3
			Loam	Low		2

Table 10. weights, classes width and ranks assigned to flood influencing factors (criteria)

3.3.2. Flood Hazard Index

The flood hazard index for the study area was derived from the selected criteria and computed through the application of the weighted linear combination technique in ArcGIS environment.

This technique is grounded on the principle of a weighted average, wherein criteria with continuous attributes are first standardised to a uniform numeric scale and subsequently combined through the utilisation of weighted averages (Drobne & Lisec, 2009). Weights of each criterion are determined based on their relative importance on the investigated phenomenon. To compute the total score of each criterion, the assigned weight of relative importance of each criterion is multiplied by the scale value assigned to the criterion. These weighted values are then summed across all criteria. These process is applied for all criteria using equation (10):

(10) $$\text{FHI} = \sum W_i * X_i$$

Where, FHI = flood hazard index, W_i = normalised weight of criterion i, and X_i = rank score of each class in criterion i. Hence, using the 'weighted sum' function of the 'overlay analysis' tools in 'spatial analyst tools', a flood susceptibility map for the study area was generated as the layer of flood hazard index. Equation below:

$$\text{FHI} = 0.1919 * (\text{distance to the river}) + 0.1663 * (\text{topographic wetness index})$$
$$+ 0.1473 * (\text{drainage density}) + 0.1383 * (\text{land-coverage}) + 0.1261 * (\text{rainfall})$$
$$+ 0.1181 * (\text{slope}) + 0.0671 * (\text{digital elevation model}) + 0.0449 * (\text{soil type})$$

The generate flood hazard index layer and values derived from the index were group in five qualitative classes, each representing a varying degree of study's area susceptibility to flood hazards, ranging from very low to very high susceptibility zones. The clustering of pixels into this categories was executed by the applying the 'natural break function' in ArcGIS environment to identify breakpoints that effectively delineate the qualitative classes. This method optimises the arrangement of data cluster by minimising the average deviation within class from its respective mean while simultaneously maximising the deviation between the mean of each class and the means of the other classes (Stefanidis & Stathis, 2013). Furthermore, cumulative frequency of the flood hazard index and standard deviation of each class from its mean were computed to determine optimal breaking point and delineating flood hazard zones.

3.4. Validation of flood hazard index

Precision in the information presented on flood hazard maps plays a vital role in activities associated with flood disaster mitigation and management (Mudashiru et al., 2021). Thus, it is

essential to assess the predictive capabilities of flood hazard maps in accurately depicting inundation scenarios. Various studies have employed different approaches to analysis uncertainties; and validate flood hazard maps. While some studies utilised location-based historical flood data, focusing on flood events in specified areas (Kazakis et al., 2015; Wang et al., 2011), others have relied on spatial maps derived from satellite imagery depicting historical flood events (Dash & Sar, 2020; Allafta & Opp, 2021), and physical models ((Elkhrachy, 2015)) to verify generated flood hazard maps. Although all of the above approaches possess inherent strength and limitation in term of validating the forecasting capacity of flood hazard maps, spatial maps of historical flood events derived from satellite imagery proved to effective for validating flood hazard maps, particular for regions characterised by limited local flood extent observations, spatial data scarcity and thus unavailability of inundation maps. The application of satellite remote sensing in flood detection traces its origin to the 1970s, and imagery captured by satellites and imaging systems such as NOAA (National Oceanic and Atmospheric Administration), VHRR (Very High Resolution Radiometer), AVHRR (Advanced Very High Resolution Radiometer), MODIS (Moderate Resolution Imaging Spectroradiometer) Radarsat, SAR (Synthetic-aperture radar), TerraSAR-X and Sentinel-1 have consistently served as invaluable source of data for detecting flood water and analysing inundation extent (S. Li et al., 2018).

In the current study, satellite imagery from Visible Infrared Imaging Radiometer Suite (VIIRS) have been used to extract surface water and maximum inundation extent for the study area. VIIRS proved to be superior to other satellite such as MODIS, particularly its robust flooding detection capability (www.nesdis.noaa.gov).

By applying one of the functions in imagery gallery in ArcGIS Pro, the Modified Normalised Difference Vegetation Index (MNDVI) for the study area was computed using the following satellite Imagery: NOAA-20/VIIRS (1.9.10.2020/19.10.2021/21.10.2022). the Modified Normalised Difference Vegetation Index is defined by "MNDVI = (c.NIR-Red)/(c.NIR+Red). c is a real number, which generally takes values between 0.1 and 10. NIR and Red are the reflectance at the Near Infrared and Red channels, respectively" (Skianis et al., 2009). This index is particularly efficient and useful in extracting surface water detected by satellite sensors. Therefore, by selecting the green band index and the shortwave infrared band index from of the satellite images of the study area for each of three period mentioned, the surface water extent was targeted. Consequently, using unsupervised classification technique, different pixels values were transformed into binary form with inundated areas equating to 1,

and areas not inundated equating to 0. The results obtained was converted into vector layer. Following the exclusion of permanent water bodies, the inundations maps for the three different years were integrated together forming a cumulative inundation map. The integration of the three years inundation maps and generation of a cumulative map was undertaken using a straightforward technique, whereby area that have experienced inundation at least once in either 2020, 2021 or 2022 are marked as flooded areas in the cumulative, while areas that haven't experienced inundation in any of the three years are marked as non-flood areas. Subsequently, the composite layer showcasing maximum flood extent was cross tabulated with the flood hazard map wherein, the overlap between the two layers–flood hazard susceptibility map and maximum flood extent–was computed and cross-tabulated, taking in to account the flood extent within each zone outlined flood susceptibility map.

4. RESULTS

4.1. Flood Hazard mapping

Flood hazard mapping is an approach used to determine the spatial extent of inundation under flood scenarios. This is accomplished through the analysis of multiple parameters recognised as influential in flood occurrence based on their contributions to flood phenomena. This study examines the potential geographic extent of flood hazard in Upper Nile state, taking into account eight different flood influencing factors i.e., distance to rivers, topographic wetness index, drainage density, land-coverage, rainfall, digital elevation model, slope, and soil types. These factors were evaluated and mapped using ArcGIS Pro 3.1 software to illustrate that: distance to rivers, which determines the effective infiltration zones (Vaddiraju & Talari, 2022); topographic wetness index, which determines water accumulation trend; drainage density, which dictates the partition of surface runoff and infiltration rate (Allafta & Opp, 2021); land-coverage, which influences recharge processes; rainfall, a principal water source; elevation, which mainly influences the direction of overflow and water depth; slope, which regulates the intensity of surface runoff; and soil type, which dictates infiltration rate, have a notable influence on the evolution of flood hazards and can be holistically analysed to determine the potential geographic extent of flood hazards.

4.2. Flood influencing factors

4.2.1. Distance to Rivers

The occurrence of flood is proportionately linked to drainage channels overflow, mainly due to capacity issue of channels. Based on the distribution of channel networks, areas in close proximity to the channels becomes more vulnerable to flood hazards and easily flooded in comparison to remote regions. In the survey conducted, the criterion 'distance to rivers' was found to be the most important flood influencing factor, assigned a relative weight of significance which equates to 19.19%. According to the classification of the thematic layer, areas within a range of 0 – 14 and 14 – 28 kilometres from perennial river networks in the study area have a high potential of flooding. Conversely, areas situated at a range between 42 – 56, and beyond 56 kilometres from the river networks have a lower probability of

experiencing inundation during flood events (Figure 7 (a & b)). Approximately 54% of the study area is situated within the proximity range of 0 – 14 kilometres from perennial water bodies, specifically, the White Nile, the Sobat and its tributaries within the study area (river Pibor and Baro), Doleib, Bibban, El-Samaa, Wehfet, Adar, Yale, Tombak, Yabus, Daga, and river Nyanding; 28% in the 14 – 28 kilometres range; 14% in the 28 – 42 kilometres range; 3% in the 42 – 56 kilometres range; and 1% in range exceeding 56 kilometres (Table 10).

4.2.2. Topographic Wetness Index

Topographic wetness index describes water accumulation trend in a particular region and the spatial distribution of wet and dry areas based on terrain's slope, elevation, and the availability of water courses. In general, a high topographic wetness index corresponds to an increased presence of surface moisture, thereby amplifying a region's vulnerability to inundation due to a reduced rate of infiltration on wet terrain. Conversely, a low topographic wetness index donates a drier surface and therefore, a low vulnerability to inundation in the event of flooding due to the capacity of drier surface to facilitate water infiltration. Based on experts' opinion, the TWI layer was assigned a relative weight of importance that equates to 16.63%. Using natural breaks, the TWI layer was classified into 5 distinctive classes (Table 10). The first class spanning on a range between 07.25 and 12.5 donates low influence on flood occurrence. Subsequently, the range extending from 12.5 to 14.5 indicates a low influence, followed by the interval between 14.5 and 16.5, which signifies a moderate influence on flood occurrence. The subsequent range, 16.5 to 18.5 indicates a high influence, while the last range, 18.5 to 34.14 indicates a very high influence on flood occurrence (Figure 7(c & d)). About 46% of the study area have a topographic wetness index value that equates to the very low-class range, i.e., 07.25 to 12.5; 23% in the low range; 14% in the moderate range; 10% in the high range' and 7% in the very high range.

4.2.3. Drainage Density

An elevated surface runoff rate mostly leads to flood occurrence, a correlation that is closely linked to high value of drainage density in a given basin. Flood occurrences are notably associated with drainage areas and peak discharge, both which are regulated by the density of the drainage systems. A high-density value of drainage system indicates more excess surface runoff, consequently amplifying the likelihood of flood incident. Conversely, a low value has a low influence on the occurrence of flood events. The study area was found to have drainage

density value ranging from 0.28 to 1.85 kilometres^2 which was classified into five categories (Table 10). Areas corresponding to very high drainage density (1.50 – 1.85 km/km^2) constitute 17% of the study area; high (1.20 - 1.50 km//km^2) covers 54%; moderate (0.90 - 1.20 km/km^2) accounts for 22%; low (0.60 - 0.90 km/km^2) represents 5%; and very low (0.28 - 0.60 km/km^2) covers 2% of the entire study area (Figure 7 (e & f)).
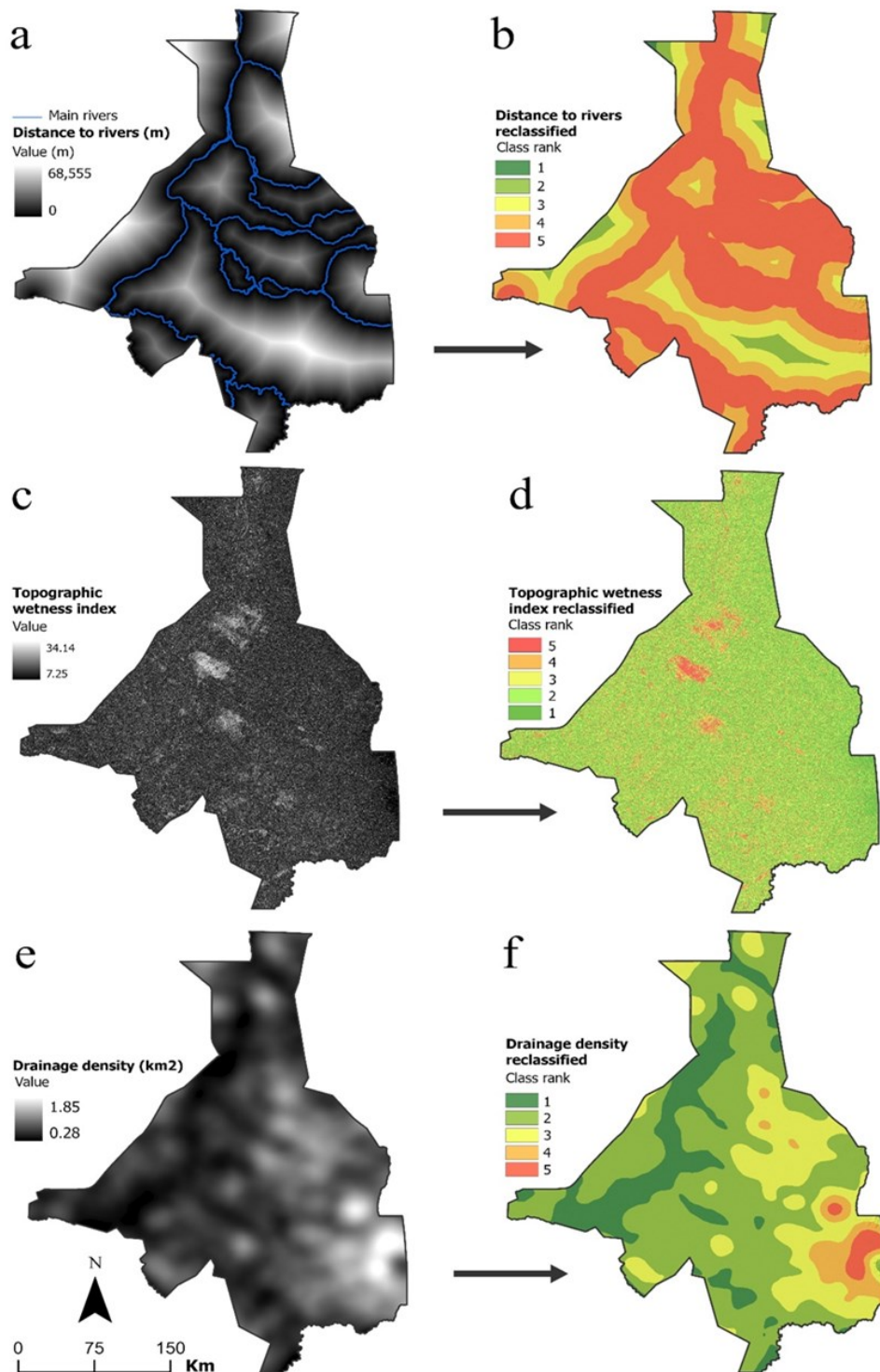
Figure 7. Thematic maps of criteria used to generate flood hazard index for the study area.

4.2.4. Land-coverage (LULC)

Land use and land cover exert a direct influence on the rate and pace of infiltration, shaping the dynamic interplay between surface and groundwater, evapotranspiration, surface runoff generation, and consequent flood events. "Impervious land cover results in infiltration capacity reduction, and runoff from such cover adds significantly to total runoff" (Allafta & Opp, 2021, p. 14). The built environment and areas characterised by prolong water presence play a notably significant role in this context. On the other hand, pervious land cover, exemplified by vegetated areas, enhances infiltration capacity, thereby establishing a negative correlation with flood occurrence. Bare land, however, exhibits a moderate influence on flood incidences, attributable to the impact of rainfall on bare land. Based on Esri's global land use/ landcover imagery portraying the land use/landcover conditions in the year 2020, the study area is characterised by 7 distinctive land classes, each systematically ranked based their respective contribution to flood incidents (Table 10). Approximately, 36% of the study area is covered by dense vegetation, an attribute that has very low flood influencing occurrence; cropland, constituting 1% of the study area, scored as a low flood-influencing attribute. Subsequently, bare land (0.7%), and pastureland (57%) are ranked as moderate flood-influencing attributes. The built environment, accounting for 0.7% of the entire study area emerges as high flood-influencing attribute due to its impact on infiltration rate and surface runoff generation. Lastly, flooded vegetation (4%) and permanent water bodies (0.6%), both ranked as having a very high influence on the occurrence of flood (Figure 8 (g & h)).

4.2.5. Rainfall

Rainfall serves as a crucial factor, directly associated with flood occurrence. The heightened intensity, frequency, and duration of precipitation, in conjunction with the topographical and hydrological attributes of a given area, have the potential to amplify the susceptibility of that region to occurrences of flooding. As shown in Table 10, the study area have a varying annual average rainfall and there is a clear distinction between the northeastern and south western part of the study (Figure 8 (j)). The general pattern of annual average rainfall in the study area shows the highest level in the western parts (1070 - 1200 mm), and the lowest level in northern parts (550 - 680 mm). Thus, the five annual average rainfall classes outlined I.e., 550 - 680, 680 - 810, 810 - 940, 940 - 1070, and 1070 - 1200 were assigned ratio score consisting of very low, low, moderate, high, and very high in the ranking of flood-influencing factors.
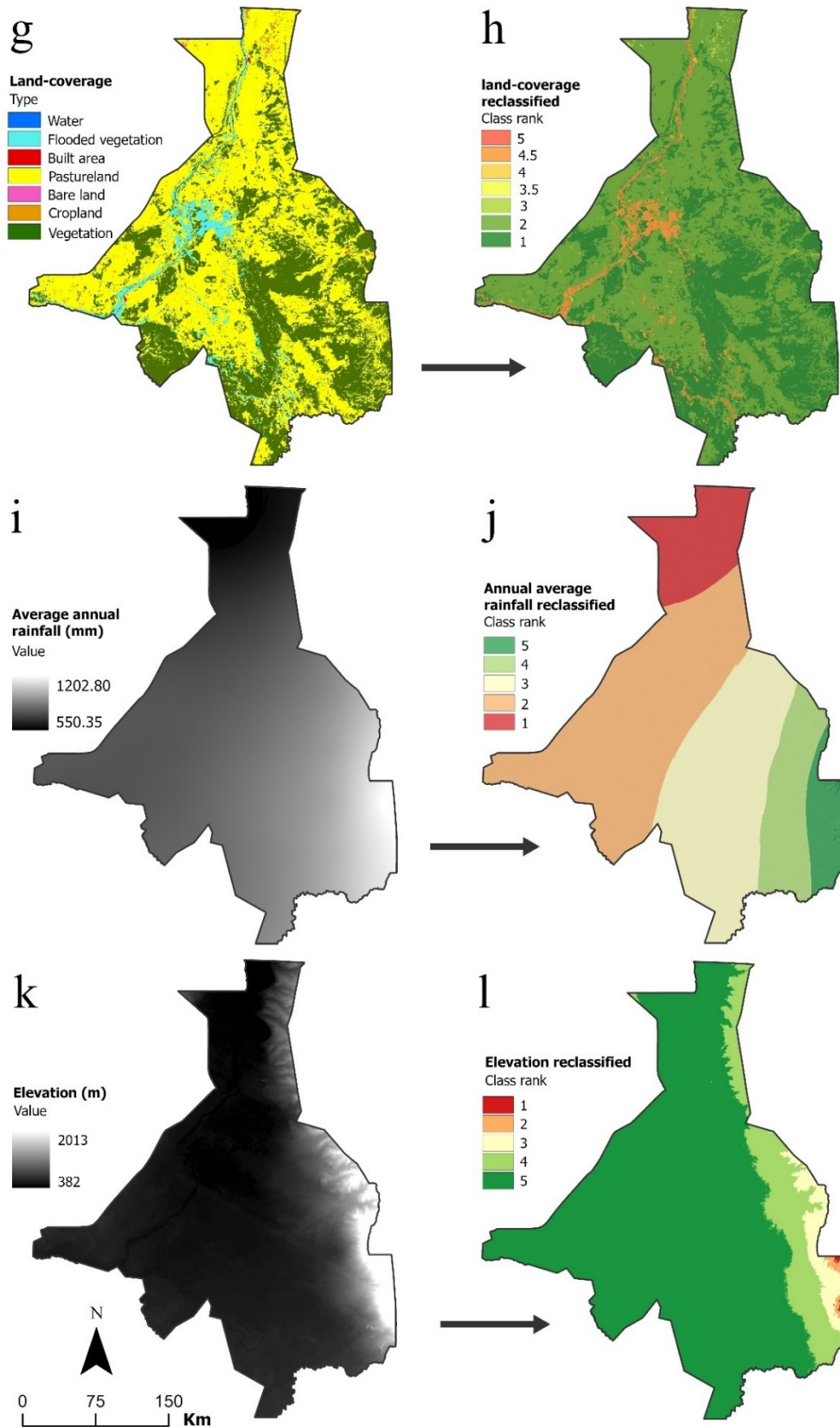
Figure 8. Thematic maps of criteria used to generate flood hazard index for the study area.

4.2.6. Elevation

Elevation exhibits an inverse correlation with flood hazards, whereby the gravitational flow of surface runoff from elevated terrain converges and gather in low-lying areas, thereby heightening their vulnerability to flood risk. The interplay of elevation significantly influences the direction, scope, and depth of flooding events. Areas characterised by lower elevations are more expose to inundation compared to areas with high elevations. This heightened exposure arises from the capacity of low-lying regions to be inundated even by floods of relatively low magnitude, attributable to the inflow of surface runoff originating areas characterised by elevated terrain. In the survey conducted with the experts, the criterion elevation was assigned a relative weight of importance amounting to 6.71% (Table 10). The terrain of the study area is primarily composed of flatland with the highest elevation reaching 2013 metres, representing a limited portion of the entire study area. In contrast, the lowest elevation is 382 metres above sea level, constituting a substantial proportion of the study area (Figure 8 (k & l)). The classes assigned to the criterion elevation is based on the natural break function whereby the class width with very high influence on flood occurrence is between 382 to 420 metres. High influence on flood occurrence is ascribe to elevations ranging from 420 to 640 metres; moderate influence pertains to elevation within the of 480 - 640 metres; low influence encompasses elevation between 640 - 970 metres; and elevation exceeding 970 metres are ranked as having a very low influence on flood occurrence (Table 10). The eastern part of the study area has the highest elevation level, therefore less prone to inundation. The central, south-western, and north-western portion of the study area, however, possess low elevations and therefore prone to inundation (Figure 8(k & l)).

4.2.7. Slope

Slope gradient, a that criterion linked to elevation of a terrain, regulates the velocity and concentration of surface runoff. The probability of flood occurrence increases inversely with the decline in the slope of region, thus rendering slope a reliable criterion in assessing the probabilistic extent of flood hazards (Rahman et al., 2019). The criterion slope was assigned a relative weight of significance that amounts to 11.81%. And similar to the rest of the criteria, the slope of the study area was classified into five distinctive classes, with each class having a varying degree of influence on the occurrence of floods, notably, areas with slope less than 1 degree, 1 - 6 degrees, 6 - 11 degrees, 11- 22 degrees, and higher than 22 degrees (Table 10).

Areas with the highest slope value and less prone to inundation are situated in the eastern part of the study area, whereas areas with varying degrees of slope that are prone to inundation are located in the central, north-western, and south-western parts of the study area (Figure 9 (m & n)).
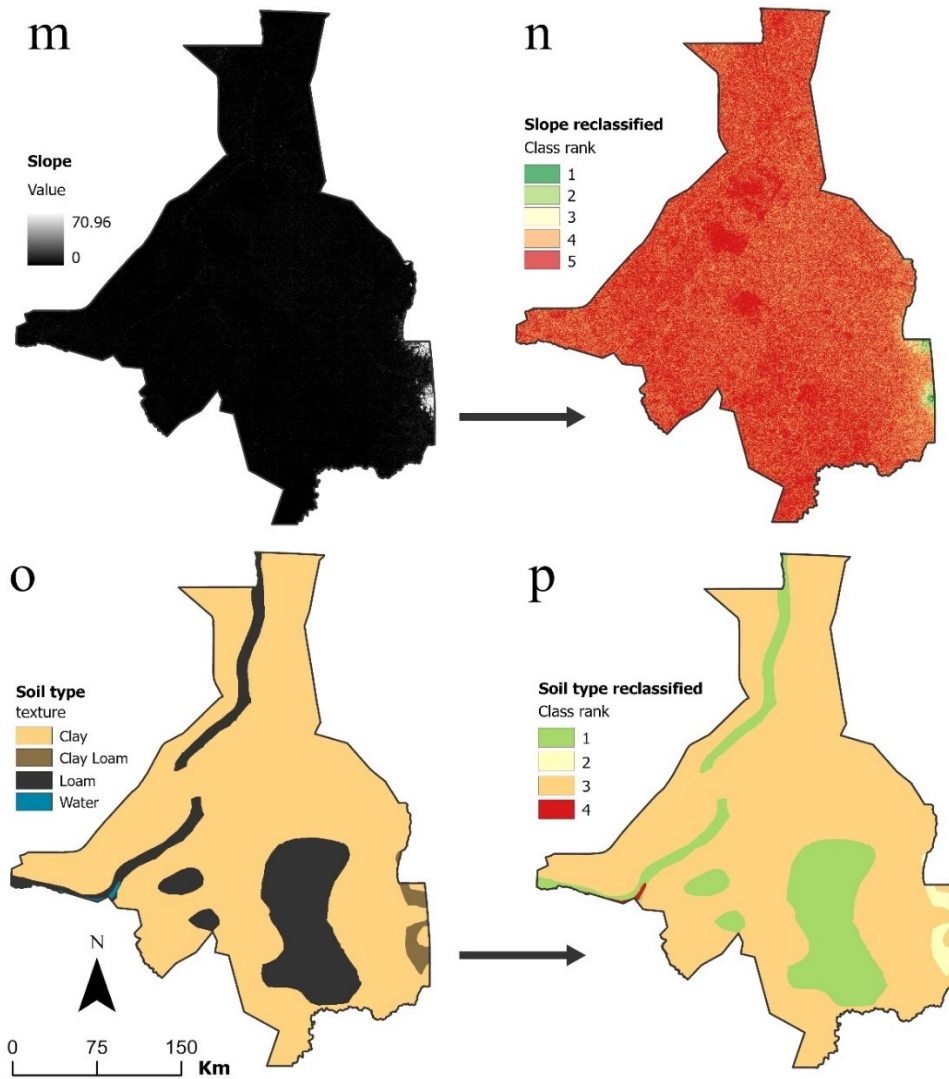
Figure 9. Thematic maps of criteria used to generate flood hazard index for the study area.

4.2.8. Soil Type

Regardless of the landcover category, infiltration rate is significantly influenced by soil type. As such, soil type determines the proneness level of an area to inundation in flood scenarios. Soil properties such as layer thickness, permeability, and infiltration rate impose a direct impact on the rainfall-runoff processes (Rimba et al., 2017). And given that different soil types have

different infiltration capacity, the probability of flood risk increases with the decrease in soil infiltration capacity and vice versa. For instance, sandy soils possess a pronounce ratio of macropores, resulting in a higher infiltration capacity and lower surface runoff in comparison to loamy soil. Loamy soils on the other hand, are characterised by high ratios of medium-sized pores which possess higher infiltration rates and lower runoff when compared to clay soil which has the highest ratio of micropores. The distribution of Soil pore size, the volume and connectivity of pores can substantially affect water transportation and the occurrence of flood. The criterion soil type for the area under investigation was categorised into four classes (i.e., clay, clay loam, loam, and water) based on the prevailing soil property of the terrain (Table 10). Approximately 18% of the study area's soil texture is of loam soil which has a low influence on the occurrence of flood hazard; 1% loam clay, which have a moderate influence level when it comes to flood hazards; 80% clay, a soil type with low infiltration rate. Areas characterised is having a watery soil texture represents less than 1% percent of the study area and have a very high level of proneness to inundation in the event of flood.

4.3. Flood hazard index

Table 10 presents the relative weights of importance of all the eight criteria used in flood hazard mapping, derived through the analytical hierarchy process. Using weighted overlay analysis in an ArcGIS environment, the eight flood influencing factors and their corresponding weights were combined, yielding a flood hazard index map for Upper Nile state (**Error! Reference source not found.**). The determined flood hazard index values fall with the range of 2.01 to 4.74. Pixels exhibiting high FHI values demonstrate greater susceptibility to flooding, whereas pixels with low FHI values exhibits low susceptibility to flooding. The FHI value were systematically classified into 5 distinct groups, each indicative of varying level of susceptibility to flood hazards (Figure 11). Pixels within the range of 2.007 to 3.046 donates areas characterised by very low susceptible level to flood hazards. Those within the range of 3.047 to 3.346 represents low susceptibility level, while values between 3.347 and 3.614 are associate with moderate susceptibility level to flood hazards. Furthermore, FHI values ranging from 3.615 to 3.914 correspond to areas exhibiting a high susceptibility level, and the range from 3.915 to 4.739 represents a notable elevation in proneness to flood hazards, signifying a very high level of susceptibility (Table 11).
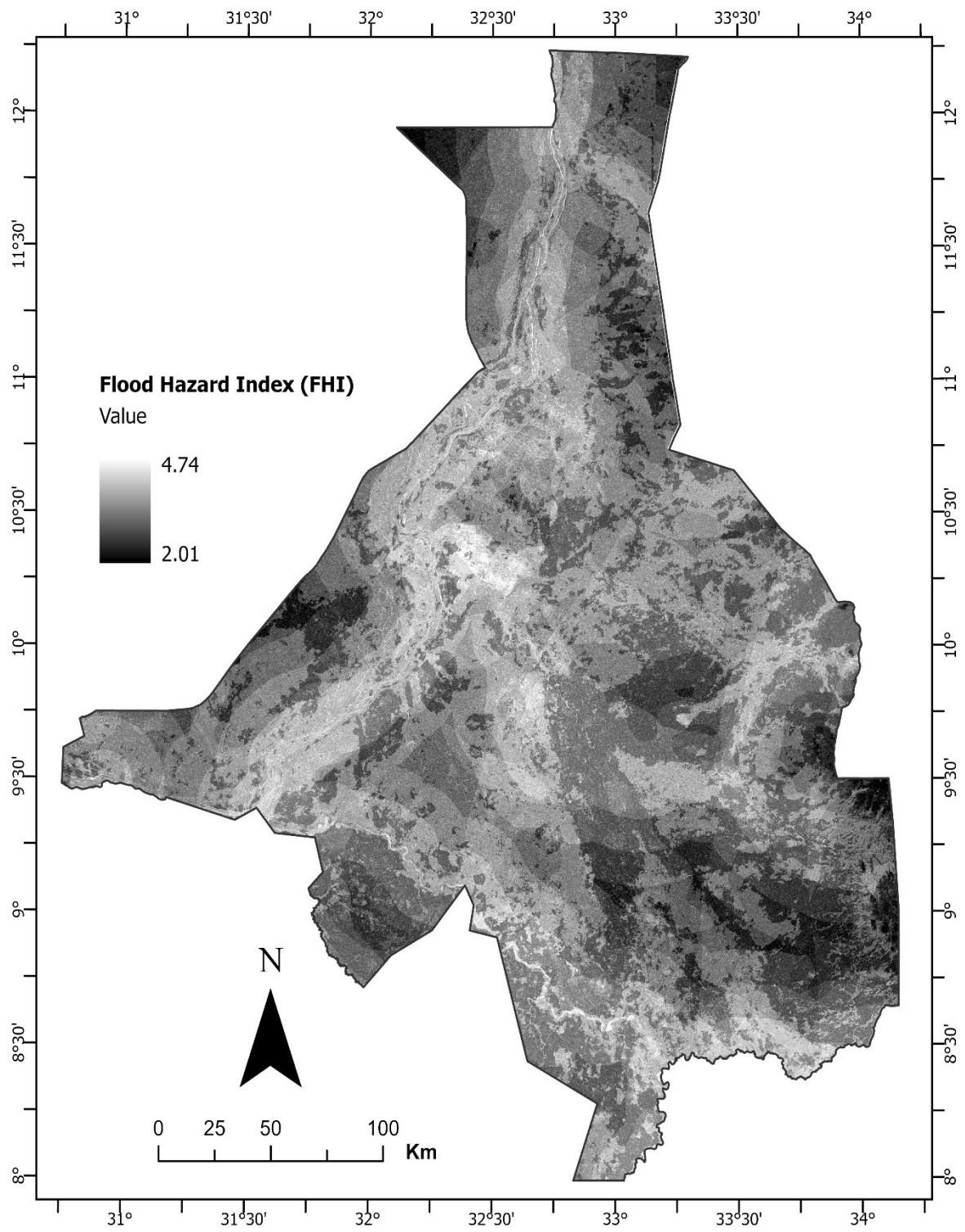
Figure 10. Digital map of the flood hazard index.

4.4. Validation results

The validity of the flood hazard model developed for Upper Nile state using GIS-based multicriteria decision analysis and the analytical hierarchy process was assessed on the basis

of historical inundation map derived from satellite imagery. The generated flood hazard map was compared to a historical inundation map illustrating the cumulative extent of floodwater in the study area during October of 2020 2021, and 2022 (Figure 12). The comparative analysis of the composite layer, representing historical inundation, and the flood hazard maps revealed distinct distributions of historical inundation extent across different flood hazard zones illustrated in the flood hazard map. Specifically, about 4% of previously inundated areas were situated within the very low zone of the flood hazard map, 16% in the low zone, 26% in the moderate zone, 32% in the high zone, and 22% in the very high zone (Figure 11).

As the validation outcomes of the flood hazard map revealed, a significant portion of the historical flood and inundation extent is concentrated within flood hazard zones classified as moderate, high, and very high susceptibility zones. About 80% of the total inundation extent observed in the preceding three years (2020, 2021, 2022) corresponds to these designated hazard zones. Consequently, the flood hazard model developed for Upper Nile state is considered satisfactory, effectively portraying areas prone to flooding and providing an accurate representation of the probabilistic extent of inundation under flood scenarios.

FHI range	Zone classification	Area		Number of cells (30x30)
		(km^2)	(%)	
2.007 - 3.046	Very low	7,222.62	9.38	7634344
3.047 - 3.346	Low	17,124.63	22.25	18071308
3.347 - 3.614	Moderate	22,548.82	29.29	23848822
3.615 - 3.914	High	20,627.40	26.80	21827321
3.915 - 4.739	Very High	9,450.65	12.28	10048305

Table 11. Classification of flood hazard zones

4.5. Flood hazard zones (FHZ)

The flood hazard index for Upper Nile state was calculated and presented in the form of flood hazards map. Employing the natural breaks' technique, FHI values were classified into five distinct hazard zones, as illustrated in Figure 11. These zones illustrate varying levels of susceptibility to flood hazards, namely very high, high, moderate, low, and very low, covering approximately 12%, 27%, 29%, 22%, and 10% of the study area, respectively (Table 11). In absolute numbers, about 9,451 kilometres square of the study area falls within the zone with a very high susceptibility level to flood hazards, 20,628 kilometres square in the zone with high susceptibility level, 22,549 kilometres square in the moderate zone, 17,125 kilometres square in the low zone, and 7,223 kilometres square in the very low zone (Table 11). Typically, areas characterised by a heightened risk of flooding are found to align with locales exhibiting

elevated runoff rates, a circumstance influenced by diverse parameters (Allafta & Opp, 2021). In the current study, zones with very high and high susceptibility level to flood hazards are situated along the major water bodies and their tributaries, particularly the White Nile River, Sobat River, and the confluence point of both rivers. Areas close to these water bodies and areas in the central part of the study area do exhibit moderate to high vulnerability to flooding, whereas the northeastern and lower-eastern part of the study area exhibit a very low and low susceptibility level to flood hazards (Figure 11). Areas characterised by a very high and high susceptibility level to flood hazards are positively affect by their proximity to perennial water bodies, elevation, slope, land use/landcover types, and the level of topographic wetness index.

Upon superimposing the land use/land cover layer onto the flood hazard index map, a discernible trend emerged, revealing a substantial proportion of the built environment situated within the moderate, high, and very high flood hazard susceptibility zones (Table 12). Specifically, urban areas and human settlement sites encompass 16.64%, 47.99%, and 33.77% within the moderate, high, and very high flood hazard susceptibility zones, respectively. Furthermore, pasturelands demonstrate an elevated vulnerability to flood events, with 15.72% of the pastureland situated within areas classified as very highly susceptible to inundation, 37.35% in the high susceptibility zone, 32.03% in the moderate zone, and 12.72% in the low susceptibility zone, accompanied by 2.15% in the very low zone. Other land use/land cover types exhibit a contrasting results in comparison to the built environment and pastureland classes. Whereby most of the bare land, agricultural areas and dense vegetation mostly situated in the very low and low flood susceptibility zones (Table 12). Precisely, 49.67% of the bare lands are within the zone classified as having a very low susceptibility level to flood hazards, while 16.13% occupies the low flood hazard susceptibility zone, 22.48% in moderate zone, 9.06% in the high, and only 2.63% in the zone with very low susceptibility level to flood hazards. On the other hand, agricultural areas in the very low, low, moderate, high, and very high flood hazards covers about 26.39%, 31.08%, 27.14%, 11.56%, and 3.80% of areas in the flood hazard index map, respectively. Similarly, the vegetation cover class is situated within 21.51%, 39.76%, 28.02%, 9.86%, and 0.83% of the respective flood hazards susceptibility zones, namely, very low, low, moderate, high, and very high flood hazards susceptibility zones, respectively.
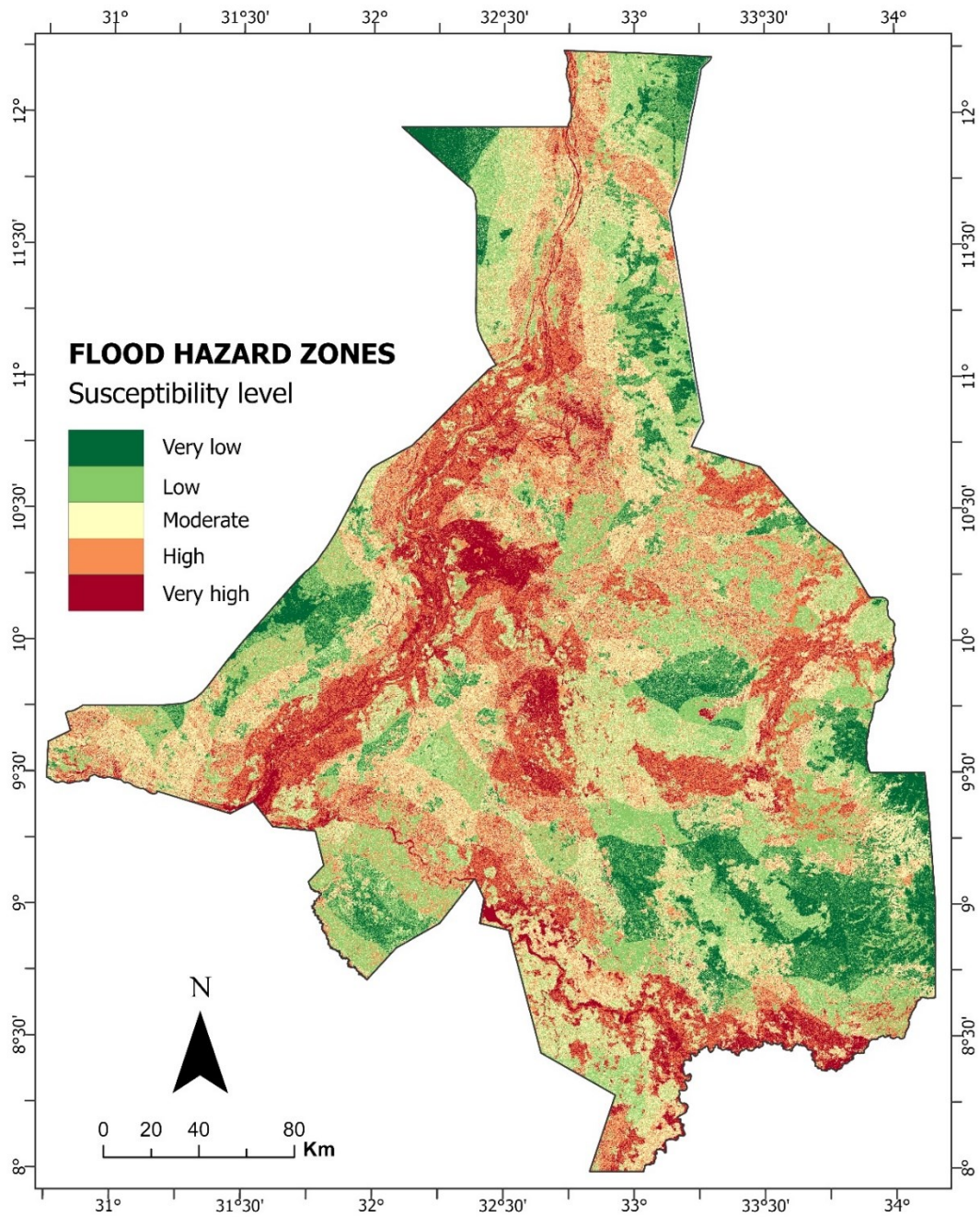
Figure 11. Flood hazard susceptibility and zoning map for Upper Nile state.

Land use/land cover	Vulnerability level									
	Very low		Low		Moderate		High		Very high	
	Km²	%	Km²	%	Km²	%	Km²	%	Km²	%
Built environment	201	0.37	665	1.22	9,108	16.65	26,258	48.00	18,474	33.77
Pastureland	957,427	2.16	5,641,668	12.72	14,208,925	32.04	16,568,977	37.36	6,972,723	15.72
Bare land	27,279	49.68	8,859	16.13	12,347	22.48	4,980	9.07	1,446	2.63
Agricultural areas	128,448	26.40	151,273	31.09	132,098	27.15	56,277	11.57	18,492	3.80
Vegetation cover	6,107,151	21.51	11,289,673	39.76	7,956,724	28.02	2,800,845	9.87	237,295	0.84

Table 12. Vulnerability of land use /landcover classes in each flood hazard zone.
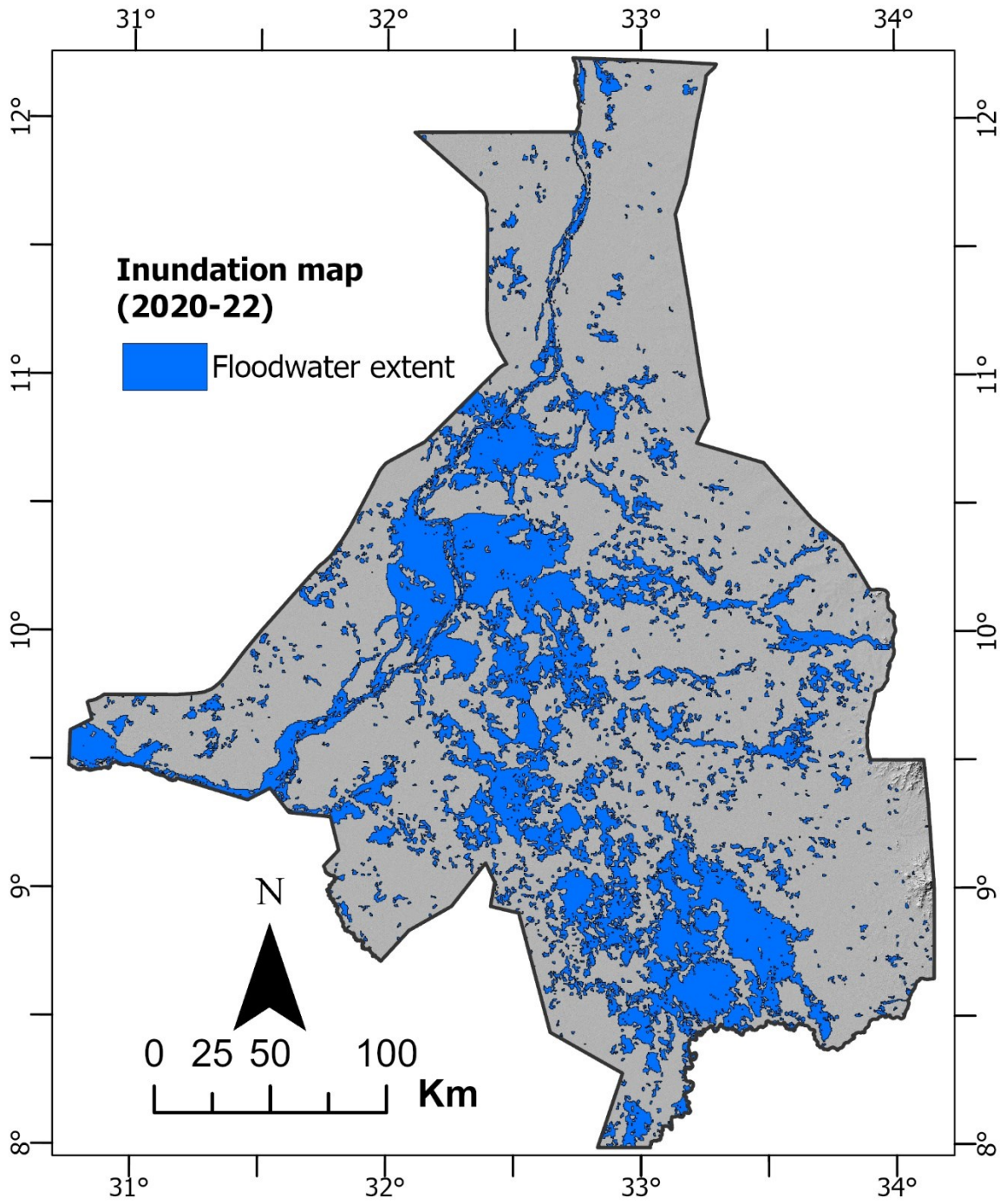
Figure 12. Satellite imagery based historical Inundation map

5. DISCUSSION

The Upper Nile state is characterised by recurrent inundation, a phenomenon documented in historical records dating as far back as the 18th century. The susceptibility of the area to flooding is heightened by its geographical positioning within a floodplain characterised by a notable variability in discharge. Additionally, the topographical attributes of the investigated area render it particularly susceptible to flooding. Consequently, this study sought out to delineate the probabilistic geographic extent of inundation under flood scenarios in the Upper Nile state, an attempt to develop flood hazard map that could be instrumental in mitigation measures to reduce the adverse effects of flooding.

Employing a methodological approach, the study utilised multicriteria decision analysis and the analytical hierarchy process, –a method deemed effective in existing literature (Kazakis et al., 2015; Ogato et al., 2020; Allafta & Opp, 2021) in delineating flood hazards zones, particularly for data-sparse, under-resourced regions of the world–in analysing and cartographically representing areas within Upper Nile state that are vulnerable to flood hazards. This was accomplished through the identification of flood influencing factors, determining their relative weight of importance in the occurrence of floods, and subsequently conducting a weighted overlay analysis in ArcGIS environment.

A total of eight flood influencing factors were selected, and their weights were determined through a survey involving experts from various fields. Among the criteria used in the flood hazard model for the study area, five were signed the highest weights of relative importance: distance to rivers having a relative wight of importance equivalent to 19.19%, topographic wetness index (16.63%), drainage density (14.73%), land use/ landcover (13.83%), rainfall (12.61%), slope (11.81%). The remaining two criteria were each assigned relative weight of importance below 10% (Table 10). Prior to the weighted overlay analysis, an assessment of the pairwise matrix's consistency was conducted. The determined consistency ratio, amounting to 2.0%, was found to be below the prescribed maximum consistency ratio of 10%, as proposed by Saaty (1990).

Using different classification technique, each criterion's value range was normalized on a scale from 1 to 5 (Table 10). Given that a large portion of floods are caused by an increase in the volume of water entering from upstream sources, primarily the Ethiopian highlands and Lake Victoria, the equal interval function was used to normalise the criterion distance to rivers

and drainage density in order to increase the number of pixels within class ranks that have a greater influence on the occurrence of floods (class rank 4 & 5), thereby partially offsetting the lack of criteria accounting for surface runoff volume and the Nile discharge.

Consequently, the eight criteria representing flood influencing factors were superimposed, generating a flood hazard index for Nile state. The Flood index Value range between 2.007 and 4.739, wherein higher values correspond to areas characterized by elevated susceptibility to flood hazards, whereas lower values denote regions less prone to such hazards. Following classification if the hazard index into five classes, each indicative of varying degrees of proneness to flood hazards, it was recognised that area along perennial water bodies more prone to flooding in comparison to areas far from water bodies. Particularly, the central and southwestern parts of the study area are represented by very high values of the flood hazard index (Figure 11). Here the effect of two criteria, namely distance to rivers and topographic wetness index is particularly revealing.

Conversely, the eastern and northeastern portions of the study area demonstrate a relatively lower proneness to flood hazards. Despite the anticipation of high flood hazard index values in these regions due to their substantial drainage density and annual rainfall patterns, the influence of those criteria was offset by elevation, land use/landcover types and the topographic wetness index level of those areas. Consequently, elevation and slope play a major role, especially in regions classified as highly susceptible to inundation.

The flood hazard index map produced was validated using satellite based historical inundation map. Imagery produced by satellite-based water detection sensors and Earth Observation (EO) plays a crucial role in determining inundation extent particularly for data-sparse regions. In this context, imagery obtained from the Visible Infrared Imaging Radiometer Suit (VIIRS) for the years 2020, 2021, and 2022, corresponding to instances of severe inundations in the study area were analysed and cross tabulated with the flood hazard index map (Figure 12). The results from the validation analysis revealed that a substantial proportion of the areas submerged in the October of 2020 2021 and 2022, approximately (80%) are within the moderate, high, and very high flood zones. Conversely, only 20% of historical inundation were in the low, and very low hazard zones.

Different land use/landcover types were found to have a varying degree of proneness to inundation (Table 12). Notably, 98% of areas denoted as built environment – representing urban areas and human settlements – are within the moderate, high, and very high flood hazard susceptibility zones. While this study did not incorporate an analysis of the population

exposed to the threat of flood hazards, from this results, this finding suggests that substantial proportion of the population within Upper Nile state are at a high risk of inundation in the event of flooding. Another category of land use at significant risk of inundation is pasture, with 85% of pasture areas located in zones classified as exhibiting moderate, high, and very high susceptibility to flooding. This, therefore, indicates a major constraint on livelihood mechanism of the local population in the event of flooding since the most dominant economic activity in the study area revolves around animal husbandry, particularly livestock grazing. Conversely, areas characterized by vegetation cover and agricultural land exhibit lower susceptibility to inundation. The positive influence of vegetation cover on infiltration rates and its adverse impact on the correlation between surface and groundwater are inversely related to the occurrence of floods.

The application of multicriteria decision analysis and the analytical hierarchy process in the current study demonstrated an accurate depiction of areas susceptible to flood hazards. This method is widely used by researchers mainly due to its capability to handle data scarcity and its effectiveness delineating flood zones of vast regions. Studies that applied this method (see section: 1.5.3) have identified its utility, attributing its value to its subjective adaptability, ease of application, and the generation of precise outcomes.

However, it is essential to highlight that the effectiveness of this approach is predominantly contingent upon two factors: (1) accurate identification and selection of criteria, and (2) the allocation of weights to individual criteria. In the current study, the selected factors are partly based on the literature and partly on the topographical characteristics of the study area. While additional factors such as volume of surface runoff were considered in the initial phase of the research, the lack of accessible observational data on Nile discharge and other types of data has limited the criterion selection to dataset that can be freely accessed. Consequently, this limitation has significantly influenced the flood hazard modelling process.

Secondly, the role of stakeholders in crucial in allocating various weights of the identified criteria. Since the weight assignment process is quite complex and necessitates a nuanced understanding of how each identified criterion influences the occurrence of flood hazards, it is imperative to identify and select stakeholders with expertise in specific domains to facilitate the pairwise assessment of each criterion. This however, the reliance on experts' opinions, may be subjected to intellectual constraints due to the subjectivity and uncertainty.

Therefore, While the flood hazard model generated for Upper Nile State is determined satisfactory based the positive validation results, its essential to outline that other modelling

techniques can be employed in conjunction with the existing model to enhance the optimization of the analysis results. This is absolute necessary for two reasons. firstly, the conventional AHP possess inherent limitation, wherein a singular numerical value is utilized to encapsulate the decision maker's inclination toward a particular alternative during pairwise comparisons (Li et al., 2013). This approach, however, falls short in adequately capturing the nuanced opinions of decision-makers (Kahraman et al., 2003). Therefore, a more sophisticated approach that considers the nuanced perspectives of experts can be employed. Secondly, and on the basis of the utility of the flood hazard model for formulating measures to mitigate flood hazards, a less intricate approach may be employed. Given the complexity of the analytical hierarchy process and the substantial reliance on institutional capacity for the implementation of its outcomes, decision-making bodies may find it advantageous to opt for a flood hazards model developed on the basis of more straightforward and uncomplicated techniques.

6. CONCLUSION

The current study employed GIS-based multicriteria decision analysis and the analytical hierarchy process in analysing the phenomenon of flood hazard in Upper Nile state, an administrative delineate in South Sudan. The objective of the study is to examines the potential spatial extent of floodwater within the boundaries of study area during flood scenarios and develop flood hazard map that illustrate the susceptibility level of the study area to flood hazards.

The flood hazard map developed for Upper Nile state was compared against historical inundation map from satellite imagery, demonstrating effectiveness in accurately depicting areas prone inundation. In particular, high susceptible zones are located the central, south-western, and western parts of the study area, along prominent water bodies. Generally, this areas are characterised by dense network of river and stream, lowland topography, low level of topographic wetness index, and a gentle slope gradient. The comparison of the flood hazard index with land use/land cover classes showed a heightened vulnerability in built environments, including urban areas, human settlements, and pasturelands, to flood hazards. The flood hazard model developed and the AHP methodology used proved to be effective in accurately depicting the phenomenon of flood hazards in the study area. This success can be attributed to the method's inherent adaptability, straightforward application, and the generation of precise results. Hence, the flood hazard map develop is anticipated to be instrumental in developing pre-flood preparedness measures, strategies, and mitigation efforts, a judgement that is entirely contingent upon the preferences of responsible entities, particularly concerning the chosen methodology.

While the developed flood hazard model accurately depicts the probabilistic geographic extent of flood hazard in the study area, it is essential to outline that the study in essence, is preliminary in nature. It falls shorts in incorporating other aspects of flood risk assessment such as the analysis of the frequency and depth of flood hazard, including the intensity and volume of Surface runoff, as well as a detailed exposure and vulnerability analysis, all of which are crucial components of integrated flood risk management. Consequently, the study should regarded as provisional, underscoring the need for supplementary research to address these gaps. Such additional investigations are crucial to optimise the obtained results and provide a

thorough understanding of the temporal and spatial dimensions of flood phenomena in the investigated area.

7. BIBLIOGRAPHY

Abdrabo, K. I., Kantoush, S. A., Saber, M., Sumi, T., Habiba, O. M., Elleithy, D., & Elboshy, B. (2020). Integrated Methodology for Urban Flood Risk Mapping at the Microscale in Ungauged Regions: A Case Study of Hurghada, Egypt. *Remote Sensing*, *12*(21), 3548. https://doi.org/10.3390/rs12213548

Agustina, R. D., Putra, R. P., & Susanti, S. (2023). Mapping Greater Bandung flood susceptibility based on multi-criteria decision analysis (MCDA) using AHP method. *Environmental Earth Sciences*, *82*(15), 370. https://doi.org/10.1007/s12665-023-11062-3

Ajibade, F. O., Ajibade, T. F., Idowu, T. E., Nwogwu, N. A., Adelodun, B., Lasisi, K. H., Opafola, O. T., Ajala, O. A., Fadugba, O. G., & Adewumi, J. R. (2021). Flood-prone area mapping using GIS-based analytical hierarchy frameworks for Ibadan city, Nigeria. *Journal of Multi-Criteria Decision Analysis*, *28*(5–6), 283–295. https://doi.org/10.1002/mcda.1759

Aladejana, O., Salami, A. T., & Adetoro, O. O. (2021). Potential flood hazard zone mapping based on geomorphologic considerations and fuzzy analytical hierarchy model in a data scarce West African basin. *Geocarto International*, *36*(19), 2160–2185. https://doi.org/10.1080/10106049.2019.1687595

Allafta, H., & Opp, C. (2021). GIS-based multi-criteria analysis for flood prone areas mapping in the trans-boundary Shatt Al-Arab basin, Iraq-Iran. *Geomatics, Natural Hazards and Risk*, *12*(1), 2087–2116. https://doi.org/10.1080/19475705.2021.1955755

Arabameri, A., Rezaei, K., Cerdà, A., Conoscenti, C., & Kalantari, Z. (2019a). A comparison of statistical methods and multi-criteria decision making to map flood hazard susceptibility in Northern Iran. *Science of The Total Environment*, *660*, 443–458. https://doi.org/10.1016/j.scitotenv.2019.01.021

Arianpour, M., & Jamali, A. A. (2015). Flood Hazard Zonation using Spatial Multi-Criteria Evaluation (SMCE) in GIS (Case Study: Omidieh - Khuzestan). *European Online Journal of Natural and Social Sciences*, *4*(1), Article 1.

Bagyaraj, M., Senapathi, V., Chung, S. Y., Gopalakrishnan, G., Xiao, Y., Karthikeyan, S., Nadiri, A. A., & Barzegar, R. (2023). A geospatial approach for assessing urban flood risk zones in Chennai, Tamil Nadu, India. *Environmental Science and Pollution Research*, *30*(45), 100562–100575. https://doi.org/10.1007/s11356-023-29132-1

Bellos, V. (2012). *Ways for flood hazard mapping in urbanised environments: A short literature review*.

Berz, G. (2000). Flood disasters: Lessons from the past—worries for the future. *Proceedings of the Institution of Civil Engineers - Water and Maritime Engineering*, *142*(1), 3–8. https://doi.org/10.1680/wame.2000.142.1.3

Borzi, G., Roig, A., Tanjal, C., Santucci, L., Tejada Tejada, M., & Carol, E. (2021). Flood hazard assessment in large plain basins with a scarce slope in the Pampean Plain, Argentina. *Environmental Monitoring and Assessment*, *193*(4), 177. https://doi.org/10.1007/s10661-021-08988-1

Bunmi Mudashiru, R., Sabtu, N., Abdullah, R., Saleh, A., & Abustan, I. (2022). Optimality of flood influencing factors for flood hazard mapping: An evaluation of two multi-criteria decision-making methods. *Journal of Hydrology*, *612*, 128055. https://doi.org/10.1016/j.jhydrol.2022.128055

Carmo, J. S. A. D. (2020). *Physical Modelling vs. Numerical Modelling: Complementarity and Learning* [Preprint]. ENGINEERING. https://doi.org/10.20944/preprints202007.0753.v1

Chen, C.-T., Lin, C.-T., & Huang, S.-F. (2006). A fuzzy approach for supplier evaluation and selection in supply chain management. *International Journal of Production Economics*, *102*(2), 289–301. https://doi.org/10.1016/j.ijpe.2005.03.009

Chen, Y., Barrett, D., Liu, R., Gao, L., Zhou, M., Renzullo, L., Cuddy, S., & Emelyanova, I. (2014). A spatial framework for regional-scale flooding risk assessment. *International Environmental Modelling and Software Society (iEMSs)*. International Environmental Modelling and Software Society (iEMSs), San Deigo, CA, USA. http://www.iemss.org/society/index.php/iemss-2014-proceedings

Chen, Y., Li, J., & Xu, H. (2016). Improving flood forecasting capability of physically based distributed hydrological models by parameter optimization. *Hydrology and Earth System Sciences*, *20*(1), 375–392. https://doi.org/10.5194/hess-20-375-2016

Chundeli, F., & Kranthi, N. (2018). Flood Vulnerability Assessment using Geospatial Techniques: Chennai, India. *Indian Journal of Science and Technology*, *11*.

Churchman, C. W., Ackoff, R. L., & Arnoff, E. L. (1957). *Introduction to operations research* (pp. x, 645). Wiley.

Cirillo, G., & Albrecht, E. (2015). *The importance of law in flood risk management*. 91–102. https://doi.org/10.2495/RM150091

Collins, M. G., Steiner, F. R., & Rushman, M. J. (2001). Land-Use Suitability Analysis in the United States: Historical Development and Promising Technological Achievements. *Environmental Management*, *28*(5), 611–621. https://doi.org/10.1007/s002670010247

Corvacho-Ganahín, O., González-Pacheco, M., Francos, M., & Carvalho, F. (2023). Evaluation of potential flood hazard through spatial zoning in Acha–Arica, northern Chile, integrating GIS, multi-criteria analysis and two-dimensional numerical simulation. *Natural Hazards*, *118*(1), 755–783. https://doi.org/10.1007/s11069-023-06027-5

Costache, R. (2019). Flood Susceptibility Assessment by Using Bivariate Statistics and Machine Learning Models—A Useful Tool for Flood Risk Management. *Water Resources Management*, *33*(9), 3239–3256. https://doi.org/10.1007/s11269-019-02301-z

Dano, U., Balogun, A.-L., Matori, A.-N., Wan Yusouf, K., Abubakar, I., Said Mohamed, M., Aina, Y., & Pradhan, B. (2019). Flood Susceptibility Mapping Using GIS-Based Analytic Network Process: A Case Study of Perlis, Malaysia. *Water*, *11*(3), 615. https://doi.org/10.3390/w11030615

Danso, S. Y., Ma, Y., Adjakloe, Y. D. A., & Addo, I. Y. (2020). Application of an Index-Based Approach in Geospatial Techniques for the Mapping of Flood Hazard Areas: A Case of Cape Coast Metropolis in Ghana. *Water*, *12*(12), Article 12. https://doi.org/10.3390/w12123483

Dash, P., & Sar, J. (2020). Identification and validation of potential flood hazard area using GIS-based multi-criteria analysis and satellite data-derived water index. *Journal of Flood Risk Management*, *13*(3), e12620. https://doi.org/10.1111/jfr3.12620

de Brito, M. M., & Evers, M. (2016). Multi-criteria decision-making for flood risk management: A survey of the current state of the art. *Natural Hazards and Earth System Sciences*, *16*(4), 1019–1033. https://doi.org/10.5194/nhess-16-1019-2016

Degiorgis, M., Gnecco, G., Gorni, S., Roth, G., Sanguineti, M., & Taramasso, A. C. (2012). Classifiers for the detection of flood-prone areas using remote sensed elevation data. *Journal of Hydrology*, *470–471*, 302–315. https://doi.org/10.1016/j.jhydrol.2012.09.006

Devia, G. K., Ganasri, B. P., & Dwarakish, G. S. (2015). A Review on Hydrological Models. *Aquatic Procedia*, *4*, 1001–1007. https://doi.org/10.1016/j.aqpro.2015.02.126

Drobne, S., & Lisec, A. (2009). Multi-attribute Decision Analysis in GIS: Weighted Linear Combination and Ordered Weighted Averaging. *Informatica*, *33*(4), 459–474.

Ekmekcioğlu, Ö., Koc, K., & Özger, M. (2021). Stakeholder perceptions in flood risk assessment: A hybrid fuzzy AHP-TOPSIS approach for Istanbul, Turkey. *International Journal of Disaster Risk Reduction*, *60*, 102327. https://doi.org/10.1016/j.ijdrr.2021.102327

Elkhrachy, I. (2015). Flash Flood Hazard Mapping Using Satellite Images and GIS Tools: A case study of Najran City, Kingdom of Saudi Arabia (KSA). *The Egyptian Journal of Remote Sensing and Space Science*, *18*(2), 261–278. https://doi.org/10.1016/j.ejrs.2015.06.007

Enomah, L. D., Downs, J., Mbaigoto, N., Fonda, B., & Umar, M. (2023). Flood risk assessment in Limbe (Cameroon) using a GIS weighed sum method. *Environment, Development and Sustainability*. https://doi.org/10.1007/s10668-023-03836-3

Evans-Pritchard, E. E. (1940). *The Nuer: A description of the modes of livelihood and political institutions of a Nilotic people*. https://www.africabib.org/rec.php?RID=051316609

FAO, L. and W. D. (2011). *Land Cover Atlas of the Republic of South Sudan*. FAO. https://www.fao.org/documents/card/en/c/cc6e5ce5-bbde-4608-b2ac-1d5a6f5042cd

Feloni, E., Mousadis, I., & Baltas, E. (2020). Flood vulnerability assessment using a GIS-based multi-criteria approach—The case of Attica region. *Journal of Flood Risk Management*, *13*(S1), e12563. https://doi.org/10.1111/jfr3.12563

Fernández, D. S., & Lutz, M. A. (2010). Urban flood hazard zoning in Tucumán Province, Argentina, using GIS and multicriteria decision analysis. *Engineering Geology*, *111*(1–4), 90–98. https://doi.org/10.1016/j.enggeo.2009.12.006

Franci, F., Bitelli, G., Mandanici, E., Hadjimitsis, D., & Agapiou, A. (2016). Satellite remote sensing and GIS-based multi-criteria analysis for flood hazard mapping. *Natural Hazards*, *83*(1), 31–51. https://doi.org/10.1007/s11069-016-2504-9

Gigović, L., Pamučar, D., Bajić, Z., & Drobnjak, S. (2017). Application of GIS-Interval Rough AHP Methodology for Flood Hazard Mapping in Urban Areas. *Water*, *9*(6), Article 6. https://doi.org/10.3390/w9060360

Glenn, E. P., Morino, K., Nagler, P. L., Murray, R. S., Pearlstein, S., & Hultine, K. R. (2012). Roles of saltcedar (Tamarix spp.) and capillary rise in salinizing a non-flooding terrace on a flow-regulated desert river. *Journal of Arid Environments*, *79*, 56–65. https://doi.org/10.1016/j.jaridenv.2011.11.025

Goepel, K. D. (2013, June 23). *Implementing the Analytic Hierarchy Process as a Standard Method for Multi-Criteria Decision Making in Corporate Enterprises – a New AHP Excel Template with Multiple Inputs*. The International Symposium on the Analytic Hierarchy Process. https://doi.org/10.13033/isahp.y2013.047

Goes, B. J. M. (2022). Review: Assessment of the aquifers in South Sudan with a focus on Lakes State. *Hydrogeology Journal*, *30*(4), 1035–1053. https://doi.org/10.1007/s10040-022-02483-8

Gupta, L., & Dixit, J. (2022). A GIS-based flood risk mapping of Assam, India, using the MCDA-AHP approach at the regional and administrative level. *Geocarto International*, *37*(26), 11867–11899. https://doi.org/10.1080/10106049.2022.2060329

Ha, H., Bui, Q. D., Nguyen, H. D., Pham, B. T., Lai, T. D., & Luu, C. (2023). A practical approach to flood hazard, vulnerability, and risk assessing and mapping for Quang Binh province, Vietnam. *Environment, Development and Sustainability*, *25*(2), 1101–1130. https://doi.org/10.1007/s10668-021-02041-4

Hagos, Y. G., Andualem, T. G., Yibeltal, M., & Mengie, M. A. (2022). Flood hazard assessment and mapping using GIS integrated with multi-criteria decision analysis in upper Awash River basin, Ethiopia. *Applied Water Science*, *12*(7), 148. https://doi.org/10.1007/s13201-022-01674-8

Hamlat, A., Kadri, C. B., Guidoum, A., & Bekkaye, H. (2021). Flood hazard areas assessment at a regional scale in M'zi wadi basin, Algeria. *Journal of African Earth Sciences*, *182*, 104281. https://doi.org/10.1016/j.jafrearsci.2021.104281

Harris, I., Osborn, T. J., Jones, P., & Lister, D. (2020). Version 4 of the CRU TS monthly high-resolution gridded multivariate climate dataset. *Scientific Data*, *7*(1), 109. https://doi.org/10.1038/s41597-020-0453-3

Harvey, C. P. D. (1982). The archaeology of the Southern Sudan: Environmental context. In *CULTURE HISTORY IN THE SOUTHERN SUDAN ARCHAEOLOGY, LINGUISTICS AND ATHNOHISOTRY* (p. 189). British Institute in Eastern Africa.

Hassan, F. (2007). Extreme Nile Floods and Famines in Medieval Egypt (AD 930-1500) and Their Climatic Implications. *Quaternary International*, *173–174*, 101–112. https://doi.org/10.1016/j.quaint.2007.06.001

Hategekimana, Y., Yu, L., Nie, Y., Zhu, J., Liu, F., & Guo, F. (2018). Integration of multi-parametric fuzzy analytic hierarchy process and GIS along the UNESCO World Heritage: A flood hazard index, Mombasa County, Kenya. *Natural Hazards*, *92*(2), 1137–1153. https://doi.org/10.1007/s11069-018-3244-9

HIRABAYASHI, Y., KANAE, S., EMORI, S., OKI, T., & KIMOTO, M. (2008). Global projections of changing risks of floods and droughts in a changing climate. *Hydrological Sciences Journal*, *53*(4), 754–772. https://doi.org/10.1623/hysj.53.4.754

Hirabayashi, Y., Tanoue, M., Sasaki, O., Zhou, X., & Yamazaki, D. (2021). Global exposure to flooding from the new CMIP6 climate model projections. *Scientific Reports*, *11*(1), Article 1. https://doi.org/10.1038/s41598-021-83279-w

Hong, H., Tsangaratos, P., Ilia, I., Liu, J., Zhu, A.-X., & Chen, W. (2018). Application of fuzzy weight of evidence and data mining techniques in construction of flood susceptibility map of Poyang County, China. *Science of The Total Environment*, *625*, 575–588. https://doi.org/10.1016/j.scitotenv.2017.12.256

HORTON, R. E. (1945). EROSIONAL DEVELOPMENT OF STREAMS AND THEIR DRAINAGE BASINS; HYDROPHYSICAL APPROACH TO QUANTITATIVE MORPHOLOGY. *GSA Bulletin*, *56*(3), 275–370. https://doi.org/10.1130/0016-7606(1945)56[275:EDOSAT]2.0.CO;2

Household Economic Analysis (HEA). Livelihood Profiles- South Sudan Eastern Flood Plains & Nile and Sobat Rivers. (2013). UNHCR Operational Data Portal (ODP). https://data.unhcr.org/en/documents/details/28976

Hurst, H. E. (1920). Short Report on Nile Gauge Readings and Discharges (No. 1). *Government Press (Cairo)*.

Islam, R., Kamaruddin, R., Ahmad, S. A., Jan, S. J., & Anuar, A. R. (2016). *A Review on Mechanism of Flood Disaster Management in Asia*. *6*(1).

Johnson, D. H. (1986). The Historical Approach to the Study of Societies and their Environment in the Eastern Upper Nile Plains. *Cahiers d'études Africaines*, *26*(101), 131–144. https://doi.org/10.3406/cea.1986.2169

Johnson, D. H. (1989). *Political Ecology in the Upper Nile: The Twentieth Century Expansion of the Pastoral 'Common Economy'*. https://www.jstor.org/stable/182919

Johnson, D. H. (1992). Reconstructing a History of Local Floods in the Upper Nile Region of the Sudan. *The International Journal of African Historical Studies*, *25*(3), 607–649. https://doi.org/10.2307/219027

Johnson, D. H. (2019). Adaptation to floods in the Jonglei area of the Sudan: An historical analysis. In D. H. Johnson & D. M. Anderson (Eds.), *The Ecology of Survival* (1st ed., pp. 173–192). Routledge. https://doi.org/10.4324/9780429310249-9

Kahraman, C., Ruan, D., & Doğan, I. (2003). Fuzzy group decision-making for facility location selection. *Information Sciences*, *157*, 135–153. https://doi.org/10.1016/S0020-0255(03)00183-X

Kanani-Sadat, Y., Arabsheibani, R., Karimipour, F., & Nasseri, M. (2019). A new approach to flood susceptibility assessment in data-scarce and ungauged regions based on GIS-based hybrid multi criteria decision-making method. *Journal of Hydrology*, *572*, 17–31. https://doi.org/10.1016/j.jhydrol.2019.02.034

Karra, K., Kontgis, C., Statman-Weil, Z., Mazzariello, J. C., Mathis, M., & Brumby, S. P. (2021). Global land use / land cover with Sentinel 2 and deep learning. *2021 IEEE International Geoscience and Remote Sensing Symposium IGARSS*, 4704–4707. https://doi.org/10.1109/IGARSS47720.2021.9553499

Kazakis, N., Kougias, I., & Patsialis, T. (2015). Assessment of flood hazard areas at a regional scale using an index-based approach and Analytical Hierarchy Process: Application in Rhodope–Evros region, Greece. *Science of The Total Environment*, *538*, 555–563. https://doi.org/10.1016/j.scitotenv.2015.08.055

Kelleher, C., & McPhillips, L. (2020). Exploring the application of topographic indices in urban areas as indicators of pluvial flooding locations. *Hydrological Processes*, *34*(3), 780–794. https://doi.org/10.1002/hyp.13628

Khaleghi, S., & Mahmoodi, M. (2017). Assessment of flood hazard zonation in a mountainous area based on gis and analytical hierarchy process. *Carpathian Journal of Earth and Environmental Sciences*, *12*, 311–322.

Khosravi, K., Shahabi, H., Pham, B. T., Adamowski, J., Shirzadi, A., Pradhan, B., Dou, J., Ly, H.-B., Gróf, G., Ho, H. L., Hong, H., Chapi, K., & Prakash, I. (2019). A comparative assessment of flood susceptibility modeling using Multi-Criteria Decision-Making Analysis and Machine Learning Methods. *Journal of Hydrology*, *573*, 311–323. https://doi.org/10.1016/j.jhydrol.2019.03.073

Kim, T. H., Kim, B., & Han, K.-Y. (2019). Application of Fuzzy TOPSIS to Flood Hazard Mapping for Levee Failure. *Water*, *11*(3), 592. https://doi.org/10.3390/w11030592

Kourgialas, N. N., & Karatzas, G. P. (2011). Flood management and a GIS modelling method to assess flood-hazard areas—A case study. *Hydrological Sciences Journal*, *56*(2), 212–225. https://doi.org/10.1080/02626667.2011.555836

Kundzewicz, Z. W., Kanae, S., Seneviratne, S. I., Handmer, J., Nicholls, N., Peduzzi, P., Mechler, R., Bouwer, L. M., Arnell, N., Mach, K., Muir-Wood, R., Brakenridge, G. R., Kron, W., Benito, G., Honda, Y., Takahashi, K., & Sherstyukov, B. (2014). Flood risk and climate change: Global and regional perspectives. *Hydrological Sciences Journal*, *59*(1), 1–28. https://doi.org/10.1080/02626667.2013.857411

Le Cozannet, G., Garcin, M., Bulteau, T., Mirgon, C., Yates, M. L., Méndez, M., Baills, A., Idier, D., & Oliveros, C. (2013). An AHP-derived method for mapping the physical vulnerability of coastal areas at regional scales. *Natural Hazards and Earth System Sciences*, *13*(5), 1209–1227. https://doi.org/10.5194/nhess-13-1209-2013

Lee, G., Jun, K. S., & Chung, E.-S. (2014). Robust spatial flood vulnerability assessment for Han River using fuzzy TOPSIS with α-cut level set. *Expert Systems with Applications*, *41*(2), 644–654. https://doi.org/10.1016/j.eswa.2013.07.089

Levy, J. K. (2005). Multiple criteria decision making and decision support systems for flood risk management. *Stochastic Environmental Research and Risk Assessment*, *19*(6), 438–447. https://doi.org/10.1007/s00477-005-0009-2

Li, F., Phoon, K. K., Du, X., & Zhang, M. (2013). Improved AHP Method and Its Application in Risk Identification. *Journal of Construction Engineering and Management*, *139*(3), 312–320. https://doi.org/10.1061/(ASCE)CO.1943-7862.0000605

Li, S., Sun, D., Goldberg, M. D., Sjoberg, B., Santek, D., Hoffman, J. P., DeWeese, M., Restrepo, P., Lindsey, S., & Holloway, E. (2018). Automatic near real-time flood detection using Suomi-NPP/VIIRS data. *Remote Sensing of Environment*, *204*, 672–689. https://doi.org/10.1016/j.rse.2017.09.032

Lim, K.-S., & Lee, D.-R. (2009). The spatial MCDA approach for evaluating flood damage reduction alternatives. *KSCE Journal of Civil Engineering*, *13*(5), 359–369. https://doi.org/10.1007/s12205-009-0359-2

Liu, J., Xu, Z., Chen, F., Chen, F., & Zhang, L. (2019). Flood Hazard Mapping and Assessment on the Angkor World Heritage Site, Cambodia. *Remote Sensing*, *11*(1), 98. https://doi.org/10.3390/rs11010098

Liu, L., Zhou, L., Ao, T., Liu, X., & Shu, X. (2022). Flood Hazard Analysis Based on Rainfall Fusion: A Case Study in Dazhou City, China. *Remote Sensing*, *14*(19), Article 19. https://doi.org/10.3390/rs14194843

Lyons, H. G. (1907). *The Rains of the Nile Basin and the Nile Flood of 1906*. National Printing Department.

Mahmoud, S. H., & Gan, T. Y. (2018). Multi-criteria approach to develop flood susceptibility maps in arid regions of Middle East. *Journal of Cleaner Production*, *196*, 216–229. https://doi.org/10.1016/j.jclepro.2018.06.047

Malczewski, J. (1999). *GIS and Multicriteria Decision Analysis*. John Wiley & Sons.

Malczewski, J. (2006). GIS-based multicriteria decision analysis: A survey of the literature. *International Journal of Geographical Information Science*, *20*(7), 703–726. https://doi.org/10.1080/13658810600661508

Malczewski, J., & Rinner, C. (2015). *Multicriteria Decision Analysis in Geographic Information Science*. Springer Berlin Heidelberg. https://doi.org/10.1007/978-3-540-74757-4

Mayen, M., Wood, E., & Frazier, T. (2022). Practical flood risk reduction strategies in South Sudan. *Journal of Emergency Management*, *20*, 123–136. https://doi.org/10.5055/jem.0669

McHarg, I. L. (1969). *Design with Nature*. American Museum of Natural History.

Mendoza, G. A., & Martins, H. (2006). Multi-criteria decision analysis in natural resource management: A critical review of methods and new modelling paradigms. *Forest Ecology and Management*, *230*(1–3), 1–22. https://doi.org/10.1016/j.foreco.2006.03.023

Michael, A. (2006). The Encyclopedia of Natural Calamities Floods. *Viva-Facts on Life Science Library, Viva Books Private Limited, New Delhi*, 34–36.

Milly, P. C. D., Wetherald, R. T., Dunne, K. A., & Delworth, T. L. (2002). Increasing risk of great floods in a changing climate. *Nature*, *415*(6871), Article 6871. https://doi.org/10.1038/415514a

Mirza, M. M. Q. (2003). Climate change and extreme weather events: Can developing countries adapt? *Climate Policy*, *3*(3), 233–248. https://doi.org/10.3763/cpol.2003.0330

Moges, S. A., & Taye, M. T. (2019). Chapter 30 - Regional flood frequency curves for remote rural areas of the Nile River Basin: The case of Baro-Akobo drainage basin, Ethiopia. In A. M. Melesse, W. Abtew, & G. Senay (Eds.), *Extreme Hydrology and Climate Variability* (pp. 385–393). Elsevier. https://doi.org/10.1016/B978-0-12-815998-9.00030-0

Moghadas, M., Asadzadeh, A., Vafeidis, A., Fekete, A., & Kötter, T. (2019). A multi-criteria approach for assessing urban flood resilience in Tehran, Iran. *International Journal of Disaster Risk Reduction*, *35*, 101069. https://doi.org/10.1016/j.ijdrr.2019.101069

Mondlane, A., Hansson, K., & Popov, O. (2013). ICT for flood risk management strategies a GIS-based MCDA (M) approach. *2013 IST-Africa Conference & Exhibition*, 1–9. https://ieeexplore.ieee.org/abstract/document/6701787

Moon, W., & Hannachi, A. (2021). River Nile discharge, the Pacific Ocean and world climate – a seasonal synchronization perspective. *Tellus A: Dynamic Meteorology and Oceanography*, *73*(1), 1–12. https://doi.org/10.1080/16000870.2021.1947551

Morea, H., & Samanta, S. (2020). Multi-criteria decision approach to identify flood vulnerability zones using geospatial technology in the Kemp-Welch Catchment, Central Province, Papua New Guinea. *Applied Geomatics*, *12*(4), 427–440. https://doi.org/10.1007/s12518-020-00315-6

Mothapo, M. C., Tawodzera, G., & Sibanda, M. (2022). Assessment of physical vulnerability to flooding using Geographic Information System (GIS)-based Multi-Criteria Decision Analysis (MDCA) in Lephalale Local Municipality in Limpopo, South Africa. *Journal for Studies in Humanities and Social Sciences*, *11*(1 & 2), Article 1 & 2.

Mudashiru, R. B., Sabtu, N., Abustan, I., & Balogun, W. (2021). Flood hazard mapping methods: A review. *Journal of Hydrology*, *603*, 126846. https://doi.org/10.1016/j.jhydrol.2021.126846

Najibi, N., & Deviremi, N. (2018). Recent trends in the frequency and duration of global floods. *Earth System Dynamics*, *9*(2), 757–783. https://doi.org/10.5194/esd-9-757-2018

NASA, J. (2013). *NASA Shuttle Radar Topography Mission Global 1 arc second*. NASA EOSDIS Land Processes DAAC; 2022-12-10. https://doi.org/10.5067/MEaSUREs/SRTM/SRTMGL1.003

Naulin, J.-P., Payrastre, O., & Gaume, E. (2013). Spatially distributed flood forecasting in flash flood prone areas: Application to road network supervision in Southern France. *Journal of Hydrology*, *486*, 88–99. https://doi.org/10.1016/j.jhydrol.2013.01.044

Neelz, S., & Pender, G. (2013). Benchmarking of 2D Hydraulic Modelling Packages. *SC080035/SR2 Environment Agency*.

Nkwunonwo, U. C., Whitworth, M., & Baily, B. (2020). A review of the current status of flood modelling for urban flood risk management in the developing countries. *Scientific African*, *7*, e00269. https://doi.org/10.1016/j.sciaf.2020.e00269

Ogato, G. S., Bantider, A., Abebe, K., & Geneletti, D. (2020). Geographic information system (GIS)-Based multicriteria analysis of flooding hazard and risk in Ambo Town and its watershed, West shoa zone, oromia regional State, Ethiopia. *Journal of Hydrology: Regional Studies*, *27*, 100659. https://doi.org/10.1016/j.ejrh.2019.100659

Ouma, Y. O., & Tateishi, R. (2014). Urban Flood Vulnerability and Risk Mapping Using Integrated Multi-Parametric AHP and GIS: Methodological Overview and Case Study Assessment. *Water*, *6*(6), Article 6. https://doi.org/10.3390/w6061515

Öztürk, D., Yilmaz, I., & Kırbaş, U. (2021). Flood hazard assessment using AHP in Corum, Turkey. *TECNOLOGIA Y CIENCIAS DEL AGUA*, *12*(2). https://doi.org/10.24850/j-tyca-2021-02-08

Parsian, S., Amani, M., Moghimi, A., Ghorbanian, A., & Mahdavi, S. (2021). Flood Hazard Mapping Using Fuzzy Logic, Analytical Hierarchy Process, and Multi-Source Geospatial Datasets. *Remote Sensing*, *13*(23), Article 23. https://doi.org/10.3390/rs13234761

Peel, M. C., Finlayson, B. L., & McMahon, T. A. (2007). Updated world map of the Köppen-Geiger climate classification. *Hydrology and Earth System Sciences*, *11*(5), 1633–1644. https://doi.org/10.5194/hess-11-1633-2007

Persits, F. M., Ahlbrandt, T. S., Tuttle, M. L., Charpentier, R. R., Brownfield, M. E., & Takahashi, K. I. (1997). Maps showing geology, oil and gas fields and geological provinces of Africa. In *Maps showing geology, oil and gas fields and geological provinces of Africa* (USGS Numbered Series 97-470-A; Open-File Report, Vols 97-470-A). U.S. Geological Survey. https://doi.org/10.3133/ofr97470A

Pourali, S. H., Arrowsmith, C., Chrisman, N., Matkan, A. A., & Mitchell, D. (2016). Topography Wetness Index Application in Flood-Risk-Based Land Use Planning. *Applied Spatial Analysis and Policy*, *9*(1), 39–54. https://doi.org/10.1007/s12061-014-9130-2

Raaijmakers, R., Krywkow, J., & van der Veen, A. (2008). Flood risk perceptions and spatial multi-criteria analysis: An exploratory research for hazard mitigation. *Natural Hazards*, *46*(3), 307–322. https://doi.org/10.1007/s11069-007-9189-z

Rahman, M., Ningsheng, C., Islam, M. M., Dewan, A., Iqbal, J., Washakh, R. M. A., & Shufeng, T. (2019). Flood Susceptibility Assessment in Bangladesh Using Machine Learning and Multi-criteria Decision Analysis. *Earth Systems and Environment*, *3*(3), 585–601. https://doi.org/10.1007/s41748-019-00123-y

Rimba, A., Setiawati, M., Sambah, A., & Miura, F. (2017). Physical Flood Vulnerability Mapping Applying Geospatial Techniques in Okazaki City, Aichi Prefecture, Japan. *Urban Science*, *1*(1), 7. https://doi.org/10.3390/urbansci1010007

Roy, B. (1968). Classement et choix en présence de points de vue multiples. *French Journal of Computer Science and Operational Research*, *2*(8), 57–75.

Saaty, L. (1996). Decision Making with Dependence and Feedback. *The Analytic Network Process*. https://cir.nii.ac.jp/crid/1572543024696896896

Saaty, T. L. (1977). A scaling method for priorities in hierarchical structures. *Journal of Mathematical Psychology*, *15*(3), 234–281. https://doi.org/10.1016/0022-2496(77)90033-5

Saaty, T. L. (1989). Group Decision Making and the AHP. In B. L. Golden, E. A. Wasil, & P. T. Harker (Eds.), *The Analytic Hierarchy Process: Applications and Studies* (pp. 59–67). Springer. https://doi.org/10.1007/978-3-642-50244-6_4

Saaty, T. L. (1990). How to make a decision: The Analytic Hierarchy Process. *European Journal of Operational Research*, *48*, 9–26.

Saaty, T. L., & Vargas, L. G. (2012). *Models, Methods, Concepts & Applications of the Analytic Hierarchy Process* (Vol. 175). Springer US. https://doi.org/10.1007/978-1-4614-3597-6

Saputra, D. H., Feronika, I., Aisah, S. N., & Hadibasyir, H. Z. (2023). Flood susceptibility assessment using topographic wetness index in a part of brantas watershed. *AIP Conference Proceedings*, *2727*(1), 050032. https://doi.org/10.1063/5.0141393

SCHANZE, J. (2006). FLOOD RISK MANAGEMENT − A BASIC FRAMEWORK. In J. Schanze, E. Zeman, & J. Marsalek (Eds.), *Flood Risk Management: Hazards, Vulnerability and Mitigation Measures* (pp. 1–20). Springer Netherlands. https://doi.org/10.1007/978-1-4020-4598-1_1

Skianis, G., Vaiopoulos, D., & Nikolakopoulos, K. (2009). Testing the performance of the MNDVI vegetation index. *Proc SPIE*, *7472*. https://doi.org/10.1117/12.830262

Skoulding, Z. (2019). *Footnotes to Water*. Poetry Wales Press Limited.

Sonmez, O., & Bizimana, H. (2018). Flood hazard risk evaluation using fuzzy logic and weightage based combination methods in Geographic Information System (GIS). *Scientia Iranica*, *27*(2), 517–528. https://doi.org/10.24200/sci.2018.21037

Souissi, D., Zouhri, L., Hammami, S., Msaddek, M. H., Zghibi, A., & Dlala, M. (2020). GIS-based MCDM − AHP modeling for flood susceptibility mapping of arid areas, southeastern Tunisia. *Geocarto International*, *35*(9), 991–1017. https://doi.org/10.1080/10106049.2019.1566405

South Sudan—Floods (WMO, Floodlist, media) (ECHO Daily Flash of 14 August 2020)—South Sudan | ReliefWeb. (2020, August 14). https://reliefweb.int/report/south-sudan/south-sudan-floods-wmo-floodlist-media-echo-daily-flash-14-august-2020

State Profile 2013: In Comprehensive Agricultural Development Master Plan: Final Report. (2015). Japan International Cooperation Agency. https://openjicareport.jica.go.jp/pdf/12233607.pdf

Stefanidis, S., & Stathis, D. (2013). Assessment of flood hazard based on natural and anthropogenic factors using analytic hierarchy process (AHP). *Natural Hazards*, *68*(2), 569–585. https://doi.org/10.1007/s11069-013-0639-5

Team, J. I. (1953). The Equatorial Nile Project and Its Effects in the Sudan. *The Geographical Journal*, *119*(1), 33–48. https://doi.org/10.2307/1791617

Team, S. D. I. (1954). *Natural Resources and Developmental Potential in the Southern Provinces of Sudan*. https://sudanarchive.net/

Teng, J., Jakeman, A. J., Vaze, J., Croke, B. F. W., Dutta, D., & Kim, S. (2017). Flood inundation modelling: A review of methods, recent advances and uncertainty analysis. *Environmental Modelling & Software*, *90*, 201–216. https://doi.org/10.1016/j.envsoft.2017.01.006

Tien Bui, D., Hoang, N.-D., Pham, T.-D., Ngo, P.-T. T., Hoa, P. V., Minh, N. Q., Tran, X.-T., & Samui, P. (2019). A new intelligence approach based on GIS-based Multivariate Adaptive Regression Splines and metaheuristic optimization for predicting flash flood susceptible areas at high-frequency tropical typhoon area. *Journal of Hydrology*, *575*, 314–326. https://doi.org/10.1016/j.jhydrol.2019.05.046

Tiitmamer, N., Mayai, A. T., & Mai, N. H. (2018). *Climate Change and Conflicts in South Sudan*. Sudd Institute. https://www.jstor.org/stable/resrep20118

Tkach, R. J., & Simonovic, S. P. (1997). A New Approach to Multi-criteria Decision Making in Water Resources. *Journal of Geographic Information and Decision Analysis*, *1*(1), 25–44.

Vaddiraju, S. C., & Talari, R. (2022). Urban flood susceptibility analysis of Saroor Nagar Watershed of India using Geomatics-based multi-criteria analysis framework. *Environmental Science and Pollution Research*. https://doi.org/10.1007/s11356-022-24672-4

Visser, H., Petersen, A. C., & Ligtvoet, W. (2014). On the relation between weather-related disaster impacts, vulnerability and climate change. *Climatic Change*, *125*(3), 461–477. https://doi.org/10.1007/s10584-014-1179-z

Vojtek, M., Vojteková, J., Costache, R., Pham, Q. B., Lee, S., Arshad, A., Sahoo, S., Linh, N. T. T., & Anh, D. T. (2021). Comparison of multi-criteria-analytical hierarchy process and machine learning-boosted tree models for regional flood susceptibility mapping: A case study from Slovakia. *Geomatics, Natural Hazards and Risk*, *12*(1), 1153–1180. https://doi.org/10.1080/19475705.2021.1912835

Von Neumann, J., & Morgenstern, O. (1947). *Theory of games and economic behavior, 2nd rev. Ed* (pp. xviii, 641). Princeton University Press.

Wang, Y., Hong, H., Chen, W., Li, S., Pamučar, D., Gigović, L., Drobnjak, S., Bui, D. T., & Duan, H. (2018). A Hybrid GIS Multi-Criteria Decision-Making Method for Flood Susceptibility Mapping at Shangyou, China. *Remote Sensing*, *11*(1), 62. https://doi.org/10.3390/rs11010062

Wang, Y., Li, Z., Tang, Z., & Zeng, G. (2011). A GIS-Based Spatial Multi-Criteria Approach for Flood Risk Assessment in the Dongting Lake Region, Hunan, Central China. *Water Resources Management*, *25*(13), 3465–3484. https://doi.org/10.1007/s11269-011-9866-2

Wijesinghe, W. M. D. C., Mishra, P. K., Tripathi, S., Abdelrahman, K., Tiwari, A., & Fnais, M. S. (2023). Integrated Flood Hazard Vulnerability Modeling of Neluwa (Sri Lanka) Using Analytical Hierarchy Process and Geospatial Techniques. *Water*, *15*(6), Article 6. https://doi.org/10.3390/w15061212

Wu, Y., Zhong, P., Zhang, Y., Xu, B., Ma, B., & Yan, K. (2015). Integrated flood risk assessment and zonation method: A case study in Huaihe River basin, China. *Natural Hazards*, *78*(1), 635–651. https://doi.org/10.1007/s11069-015-1737-3

Yang, X., Ding, J., & Hou, H. (2013). Application of a triangular fuzzy AHP approach for flood risk evaluation and response measures analysis. *Natural Hazards*, *68*(2), 657–674. https://doi.org/10.1007/s11069-013-0642-x

Zhang, J., & Chen, Y. (2019). Risk Assessment of Flood Disaster Induced by Typhoon Rainstorms in Guangdong Province, China. *Sustainability*, *11*(10), 2738. https://doi.org/10.3390/su11102738

Zhao, W., Shi, Z., Li, S., Chen, B., Luo, X., & Pang, W. (2020). Petroleum geological characteristics and hydrocarbon accumulation patterns in the Melut Basin, South Sudan. *Arabian Journal of Geosciences*, *13*(21), 1149. https://doi.org/10.1007/s12517-020-06153-5

8. WEBLIOGRAPHY

ActionAid. (2006, October 2). Climate change, urban flooding and the rights of the urban poor in Africa. ActionAid International. https://actionaid.org/publications/2006/climate-change-urban-flooding-and-rights-urban-poor-africa

African Regional Data Cube | Digital Earth Africa. Accessed 01 march 2023, form https://www.digitalearthafrica.org/african-regional-data-cube#:~:text=The%20ARDC%20was%20a%20prototype,the%20application%20of%20this%20technology

AHP spread sheet templet. Retrieved 5 May 2023, from https://bpmsg.com/new-ahp-excel-template-with-multiple-inputs/

Data Sets—Groups and Centres. (n.d.). Retrieved 18 July 2023, from https://www.uea.ac.uk/web/groups-and-centres/climatic-research-unit/data

EM-DAT – The International Disaster Database: Centre for Research on the Epidemiology of Disaster. Accessed 12 December 2022, from https://www.emdat.be

FAO. (1974). FAO-UNESCO Soil Map of the World,1:5.000.000, UNESCO, Paris: (1977) Volume   VI, Africa. https://www.fao.org/soils-portal/data-hub/soil-maps-and-databases/faounesco-soil-map-of-the-world/en/

FEOW. (n.d.). The Upper Nile Ecoregions. Retrieved 7 July 2023, from https://www.feow.org/ecoregions/details/522

GHOACOF. (2023). Statement from the 65th Greater Horn of Africa Climate Outlook Forum (GHACOF65). https://www.icpac.net/publications/statement-from-the-65th-greater-horn-of-africa-climate-outlook-forum-ghacof65-22-august-2023-nairobi-kenya/

Hydrogeology of South Sudan. (n.d.). Retrieved 7 July 2023, from https://earthwise.bgs.ac.uk/index.php/Hydrogeology_of_South_Sudan#Climate

IRNA. (2021). Joint flood assessment report. Retrieved 2 march 2023, from https://reliefweb.int/report/south-sudan/south-sudan-longochuk-county-upper-nile-state-irna-joint-flood-assessment-report-october-2021

Sudan river Network. Retrieved 3 June 2023, from https://data.apps.fao.org/map/catalog/static/api/records/e409bb6b-2e65-435a-8d6c-73e48706e413

World digital soil map. Retrieved 10 January 2023, from https://data.apps.fao.org/map/catalog/srv/eng/catalog.search#/search?resultType=details&sortBy=relevance&any=digital%20soil%20map&fast=index&_content_type=json&from=1&to=50

VIIRS surface reflectance product (VNP09). Retrieved 06, July 2023. From

https://ladsweb.modaps.eosdis.nasa.gov/

ACKNOWLEDGEMENT

ABSTRACT

Floods are among the most ruinous of all natural hazards. Its adverse effects include damages to the physical, social, and economic structures, and disruption of livelihoods. contemporary, attributed to climate change-induced climate variations and extreme weather events, the frequency of flood occurrence has increased all around the globe. This has therefore, augmented the necessity to comprehend the spatial and temporal dimension of flood phenomena. The current study examines the spatial dimension of flood hazard in the Upper Nile state, South Sudan, a region acknowledged to be highly vulnerable to inundation, mainly due to is geographical position within a flood plain characterized by a notable variability in discharge. The objective of this investigation is to map the potential spatial extent of floodwater within the boundaries of study area under flood scenarios.

The index-based flood hazard map was developed using GIS-based multicriteria decision analysis (MCDA), and the analytical hierarchy process (AHP). Eight flood influencing factors were used in this study, namely; distance to rivers, topographic wetness index, drainage density, land-coverage (LULC), annual average rainfall, slope, elevation, and soil types. The flood hazard map developed for study area consist of five flood hazard susceptibility zones: very high, high, moderate, low, and very low. These zones encompass proportions of 12%, 26%, 29%, 22%, and 9% of the study area, respectively. The flood hazard map was further validated using satellite historical inundation map and determined to be satisfactory in depicting the probabilistic spatial extent of inundation. The flood hazard model developed is anticipated to be instrumental in pre-flood preparedness measures as well as a guide for future detailed investigations on the spatial–temporal dimension of flood incidents in the Upper Nile state.

SOMMARIO

Le alluvioni sono tra i rischi naturali più rovinosi. I loro effetti avversi comprendono danni alle strutture fisiche, sociali ed economiche, ed un deterioramento dei mezzi di sussistenza.

Allo stesso tempo, attribuito alle variazioni climatiche ed eventi estremi causati dal cambiamento climatico, è stato registrato un incremento nella frequenza di alluvioni a livello globale, aumentando la necessita di comprendere gli aspetti spazio-temporali di questi fenomeni.

Questo studio esamina la dimensione spaziale del rischio di inondazione nell'Alto Nilo, Sudan del Sud, regione con una riconosciuta vulnerabilità verso le inondazioni, causata principalmente dal suo posizionamento geografico all'interno di una pianura alluvionale caratterizzata da una notevole variabilità della portata di piena. L'obiettivo di questa indagine è quello di mappare la potenziale estensione spaziale degli allagamenti all'interno dell'area di studio in uno scenario di inondazione.

La mappa del rischio di inondazioni, fondata su diversi indici, è stata sviluppata utilizzando una decisione d'analisi multicriteriale (MCDA) basata su GIS, ed il analytical hierarchy process (AHP). Gli otto fattori d'influenza per le alluvioni utilizzati per lo studio sono: distanza da fiumi, indice di umidità topografica, densità di drenaggio, copertura del suolo (LULC), precipitazioni medie annue, pendenza, altitudine, e tipo di suolo.

La mappa del rischio di inondazione sviluppata per l'area di studio è composta da cinque zone di suscettibilità: molto alta, alta, moderata, bassa, molto bassa. Queste zone coprono rispettivamente il 12%, 26%, 29%, 22%, e 9% dell'area di studio. La mappa è stata ulteriormente validata tramite un confronto con la mappa satellitare dello storico delle inondazioni, ed è risultata soddisfacente nello stimare la probabile estensione spaziale degli allagamenti. Il modello della mappa è potrà risultare strumentale per le misure di preparazione alle inondazioni, e come guida per future indagini specifiche nella dimensione spazio-temporale di eventi alluvionali nella regione dell'Alto Nilo.

APPENDIX

Appendix 1: Multiple Input Summary Sheet of the pairwise comparison.

Expert judgement 1								
criteria	Distance to river	Topographic Wetness Index	Drainage density	Land-coverage	Rainfall	Slope	Digital Elevation Model	Soil type
Distance to rivers	**1**	1/3	1/3	1	1	3	5	9
Topographic Wetness Index	3	**1**	1	1	1	3	3	9
Drainage density	3	1	**1**	1	1	3	3	9
Land-coverage	1	1	1	**1**	1	1	3	9
Rainfall	1	1	1	1	**1**	9	3	9
Slope	1/3	1/3	1/3	1	1/9	**1**	1	5
Digital Elevation Model	1/5	1/3	1/3	1/3	1/3	1	**1**	9
Soil type	1/9	1/9	1/9	1/9	1/9	1/5	1/9	**1**

Expert judgement 2								
criteria	Distance to river	Topographic Wetness Index	Drainage density	Land-coverage	Rainfall	Slope	Digital Elevation Model	Soil type
Distance to rivers	**1**	1	1	3	1	1	9	9
Topographic Wetness Index	1	**1**	1/3	1	1/3	1	3	3
Drainage density	1	3	**1**	3	1	3	9	9
Land-coverage	1/3	1	1/3	**1**	1/3	5	9	9
Rainfall	1	3	1	3	**1**	5	7	5
Slope	1	1	1/3	1/2	1/5	**1**	7	3
Digital Elevation Model	1/9	1/3	1/9	1/9	1/7	1/7	**1**	1
Soil type	1/9	1/3	1/9	1/9	1/5	1/3	1	**1**

Expert judgement 3								
criteria	Distance to river	Topographic Wetness Index	Drainage density	Land-coverage	Rainfall	Slope	Digital Elevation Model	Soil type
Distance to rivers	**1**	1	1	1/3	1	1	7	3
Topographic Wetness Index	1	**1**	5	1	7	7	5	5
Drainage density	1	1/5	**1**	1/7	1	3	5	5
Land-coverage	3	1	7	**1**	7	7	7	7
Rainfall	1	1/7	1/2	1/7	**1**	1	5	5
Slope	1	1/7	1/3	1/7	1	**1**	3	3
Digital Elevation Model	1/7	1/5	1/5	1/7	1/5	1/3	**1**	1
Soil type	1/3	1/5	1/5	1/7	1/5	1/3	1	**1**

Expert judgement 4								
criteria	Distance to river	Topographic Wetness Index	Drainage density	Land-coverage	Rainfall	Slope	Digital Elevation Model	Soil type
Distance to rivers	**1**	1	1	1	1	1	5	5
Topographic Wetness Index	1	**1**	1/2	3	5	5	3	5
Drainage density	1	2	**1**	1	5	7	5	5
Land-coverage	1	1/3	1	**1**	1	3	1	3
Rainfall	1	1/5	1/5	1	**1**	2	3	3
Slope	1	1/5	1/7	1/3	1/2	**1**	3	3
Digital Elevation Model	1/5	1/3	1/5	1	1/3	1/3	**1**	1
Soil type	1/5	1/5	1/5	1/3	1/3	1/3	1	**1**

Expert judgement 5								
criteria	Distance to river	Topographic Wetness Index	Drainage density	Land-coverage	Rainfall	Slope	Digital Elevation Model	Soil type
Distance to rivers	**1**	1	1	3	1	1	9	9
Topographic Wetness Index	1	**1**	1/3	1	1/3	1	3	3
Drainage density	1	3	**1**	3	1	3	9	9
Land-coverage	1/3	1	1/3	**1**	1/3	2	9	9
Rainfall	1	3	1	3	**1**	5	7	5
Slope	1	1	1/3	1/2	1/5	**1**	7	3
Digital Elevation Model	1/9	1/3	1/9	1/9	1/7	1/7	**1**	1
Soil type	1/9	1/3	1/9	1/9	1/5	1/3	1	**1**

Expert judgement 6

criteria	Distance to river	Topographic Wetness Index	Drainage density	Land-coverage	Rainfall	Slope	Digital Elevation Model	Soil type
Distance to rivers	**1**	1	9	7	5	5	1	1
Topographic Wetness Index	1	**1**	3	3	5	3	1	1
Drainage density	1/9	1/3	**1**	1/3	1	1/3	1/3	1/3
Land-coverage	1/7	1/3	3	**1**	1	1	1/7	1/5
Rainfall	1/5	1/5	1	1	**1**	1	1/3	1/7
Slope	1/5	1/3	3	1	1	**1**	1	1
Digital Elevation Model	1	1	3	7	3	1	**1**	3
Soil type	1	1	3	5	7	1	1/3	**1**

Expert judgement 7

criteria	Distance to river	Topographic Wetness Index	Drainage density	Land-coverage	Rainfall	Slope	Digital Elevation Model	Soil type
Distance to rivers	**1**	1	1/3	8	3	2	5	7
Topographic Wetness Index	1	**1**	1	3	5	1/3	1	5
Drainage density	3	1	**1**	9	5	1	5	9
Land-coverage	1/8	1/3	1/9	**1**	3	1/3	1/5	1
Rainfall	1/3	1/5	1/5	1/3	**1**	1/9	1/9	9
Slope	1/2	3	1	3	9	**1**	9	9
Digital Elevation Model	1/5	1	1/5	5	9	1/9	**1**	5
Soil type	1/7	1/5	1/9	1	1/9	1/9	1/5	**1**

Expert judgement 8

criteria	Distance to river	Topographic Wetness Index	Drainage density	Land-coverage	Rainfall	Slope	Digital Elevation Model	Soil type
Distance to rivers	**1**	5	3	1	1/3	1	1	3
Topographic Wetness Index	1/5	**1**	1	1/3	1/6	1/3	1/3	1/2
Drainage density	1/3	1	**1**	1/5	1/8	1/3	1/3	1/3
Land-coverage	1	3	5	**1**	3	1	9	1
Rainfall	3	6	8	1/3	**1**	1	9	9
Slope	1	3	3	1	1	**1**	9	1
Digital Elevation Model	1	3	3	1/9	1/9	1/9	**1**	1
Soil type	1/3	2	3	1	1/9	1	1	**1**

Appendix 2. Pairwise comparison matrix of flood influencing factors (Criteria).

CRITERIA	Distance to river	Topographic Wetness Index	Drainage density	Land-coverage	Rainfall	Slope	Digital Elevation Model	Soil type
Distance to river	1	1	1 1/6	1 7/9	1 1/4	1 5/8	3 3/5	4 1/4
Topographic Wetness Index	1	1	1 1/7	1 3/8	1 3/4	1 2/3	1 5/7	2 8/9
Drainage density	6/7	7/8	1	5/6	1 2/7	1 1/2	2 1/3	3
Land-coverage	4/7	3/4	1 1/5	1	1 1/2	1 1/2	1 3/4	2 2/7
Rainfall	4/5	4/7	7/9	2/3	1	1 2/5	2	3 3/5
Slope	3/5	3/5	2/3	2/3	5/7	1	3 2/5	2 3/4
Digital Elevation Model	2/7	4/7	3/7	4/7	1/2	2/7	1	2
Soil type	1/4	1/3	1/3	3/7	2/7	1/3	1/2	1

Appendix 3. Pairwise comparison decimal matrix of flood influencing factors (Criteria).

Criteria	Distance to river	Topographic Wetness Index	Drainage density	Land-coverage	Rainfall	Slope	Digital Elevation Model	Soil type
Distance to river	1.00	1.08	1.17	1.78	1.26	1.63	3.60	4.26
Topographic Wetness Index	0.93	1.00	1.14	1.37	1.74	1.66	1.72	2.89
Drainage density	0.85	0.88	1.00	0.82	1.30	1.54	2.33	2.97
Land-coverage	0.56	0.73	1.21	1.00	1.54	1.46	1.74	2.30
Rainfall	0.79	0.57	0.77	0.65	1.00	1.39	1.94	3.60
Slope	0.62	0.60	0.65	0.69	0.72	1.00	3.39	2.76
Digital Elevation Model	0.28	0.58	0.43	0.57	0.51	0.30	1.00	2.02
Soil type	0.23	0.35	0.34	0.43	0.28	0.36	0.50	1.00